Design and Synthesis of Nonequilibrium Systems

Chuyang Cheng,[†] Paul R. McGonigal,[†,‡] J. Fraser Stoddart,[*,†] and R. Dean Astumian[*,§]

[†]Department of Chemistry, Northwestern University, 2145 Sheridan Road, Evanston, Illinois 60208, United States, [‡]Department of Chemistry, Durham University, South Road, Durham DH1 3LE, United Kingdom, and [§]Department of Physics and Astronomy, The University of Maine, Orono, Maine 04469, United States

ABSTRACT The active transport of ions and molecules across cell membranes is essential to creating the concentration gradients that sustain life in all living organisms, be they bacteria, fungi, plants, animals or *Homo sapiens*. Nature uses active transport everywhere for everything. Molecular biologists have long been attracted to the study of active transport and continue to this day to investigate and elucidate the tertiary structures of the complex motor proteins that sustain it, while physicists, interested in nonequilibrium statistical mechanics, have developed theoretical models to describe the driven ratcheting motions that are crucial to its function. The increasingly detailed understanding that contemporary science has acquired relating to active transport, however, has yet to lead to the design and construction of artificial molecular motors capable of employing ratchet-driven motions that can also perform work against concentration gradients. Mechanically interlocked molecules (MIMs) in the form of pseudo- and semirotaxanes are showing some encouraging signs in meeting these goals. This review summarizes recent progress in making artificial molecular motors that can perform work by "pumping" tetracationic rings into high-energy states. The launching pad is a bistable [2]rotaxane whose dumbbell component contains two electron-donating recognition sites, one, a tetrathiafulvalene (TTF) unit, which interacts more strongly with the ring component, cyclobis(paraquat-*p*-phenylene) ($CBPQT^{4+}$), containing two electron-accepting bipyridinium units, than does the other 1,5-dioxynaphthalene (DNP) unit. Switching can be induced electrochemically by oxidizing the TTF unit to a $TTF^{\bullet+}$ radical cation, whereupon Coulombic repulsion takes care of moving the ring to the DNP unit. Reduction of the radical cation resets the switch. Molecular switches operate at, or close to, equilibrium. Any work done during one switching event is undone during the reset. Molecular motors, on the other hand, rely on a flux of energy, and a ratchet mechanism to make periodic changes to the potential energy surface of a system in order to move molecules uphill to higher energy states. Forging a path from molecular switches to motors involved designing a molecular pump prototype. An asymmetric dumbbell with a 2-isopropylphenyl (neutral) end and a 3,5-dimethylpyridinium (charged) end with a DNP recognition site to entice $CBPQT^{4+}$ rings out of solution exhibits relative unidirectional movement of the rings with respect to the dumbbell. Redox chemistry does the trick. During the oxidative cycle, the rings enter the dumbbell by passing over the neutral end onto the recognition site; in the reduction cycle, much of the recognition is lost and the rings find their way back into solution by leaving the dumbbell from the charged end. This on-one-end, off-the-other process can be repeated over and over again using light as the energy source in the presence of a photosensitizer and a compound that shuttles electrons back and forth. Although this prototype demonstrates ratchet-driven translational motion, no work is done. A ring enters the dumbbell from one end and leaves from the other end. Another deficiency of the prototype is the fact that, although the recognition site is muted on reduction, it retains some attraction for the ring. What if the recognition site was attractive initially and then became repulsive? This question was answered by turning to radical chemistry and employing the known stabilization behavior of a bipyridinium radical cation and the bisradical dication, generated on reduction of the $CBPQT^{4+}$ ring, to pluck rings out of solution and thread them over the charged end of the pump portion of a semidumbbell. On subsequent oxidation, the pump is primed and the rings pass through a one-way door, given a little thermal energy, onto a collecting-chain where they find themselves accumulating where they would rather not be present. In this manner, an artificial molecular pump mimics the pumping machinery commonplace in biological systems. Looking beyond this state-of-the-art artificial molecular pump, we discuss, from a theoretical standpoint, the measures that would need to be taken in order to render its operation autonomous.

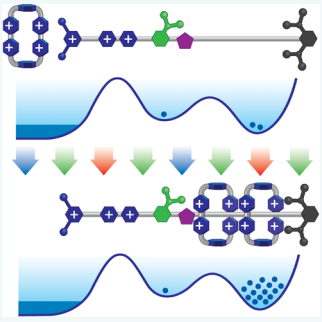

KEYWORDS: active transport · co-conformations · dissipative systems · molecular motors · mechanostereochemistry · pseudorotaxanes · radicals · ratchet mechanism · rotaxanes

It remains a formidable challenge to explain and, furthermore, to mimic the complex processes associated with life that emerge[1] when collections of molecules interact with one another to (i) dissipate energy, (ii) sustain nonequilibrium states, and (iii) perform work. In recent decades, considerable strides have been made in the scientific community's understanding[2−4] of Nature's molecular motors, which, among their many roles, are responsible[5] for creating and maintaining concentration gradients across membranes as part of cellular metabolism. The task is now laid out clearly in front of chemists to capture the essence of these molecular motors in artificial[6−15] systems (i) that are capable[6,16−18] of processing and dissipating energy, (ii) whose

* Address correspondence to stoddart@northwestern.edu, astumian@maine.edu.

Received for review June 22, 2015 and accepted July 29, 2015.

Published online July 29, 2015
10.1021/acsnano.5b03809

hierarchical organization transduces[15,19−21] movement across length scales, and ultimately (iii) that can perform[15,20−25] useful work on their environments.

For over two decades, mechanically interlocked molecules[26] (MIMs), such as rotaxanes[27,28] and catenanes,[29−31] have been a fertile playground for furthering our understanding of noncovalent bonding interactions and, hence, learning how to control large amplitude relative motions of their components. Switchable MIMs (Figure 1, upper left quadrant) that express controlled translational or circumrotational movement at the nanoscale level[19,28,32] have been created by introducing bistability into molecular shuttles[33] and employing many different pairs of recognition motifs. Typically, such molecular switches are toggled between two or more equilibrium states in response to external stimuli. For example, the minimum energy co-conformation[31] associated with the bistable [2]rotaxane[34] **R1**$^{4+}$ is adopted (Figure 2a) when its π-electron donating tetrathiafulvalene (TTF) recognition site is encapsulated within the cavity of its π-electron accepting cyclobis(paraquat-*p*-phenylene) (CBPQT^{4+}) ring component. On oxidizing the TTF unit, a new thermodynamic minimum is established in which the ring encircles the 1,5-dioxynaphthalene (DNP) recognition site in preference to the now electron poor TTF^{2+} unit. Subsequent reduction resets the switch (Figure 2b) to its initial state with random thermal noise supplying the energy necessary to overcome any energy barriers to co-conformational reorganization.[35]

There are many ways in which one can imagine exploiting these well-established molecular switches in technological settings, *e.g.*, in molecular electronic devices[36] and drug delivery systems.[37] For example, the stimulus-responsive behavior of bistable MIMs has led to them being utilized to write and store information[38] as part of sensors[39] and memory devices.[40] There is a fundamental demarcation, however, between molecular switches and Nature's biomolecular machinery, such as motor proteins and proton pumps. Molecular switches (Figure 3a) operate at, or close to, equilibrium. Any work that might be done during one switching event is subsequently undone[4,41] when the ensemble of molecules returns to its initial state.[6,15] In order for bistable switches of this ilk to perform work, regardless of how high their efficiency or positional discrimination[42] may be, they require an additional layer of complexity to be added that (i) allows their action to be coupled and uncoupled from their environment at the single molecule level, and/or (ii) imparts hierarchical order to collections of switches that act in unison. For a full discussion of these fundamental considerations, we direct readers toward previous in-depth reviews[3,6,15] on the topic. In contrast to bistable switches, the repeated actions of proton pumps and motor proteins result (Figure 3b) in the local system moving further and further away from its "inherent equilibrium", *e.g.*, by transferring protons from a region of relatively low concentration in a cell to one of higher concentration.[5] Of course, they are only able to carry out this act when there is flux of energy through the system. They do not violate the

VOCABULARY: Co-conformational rearrangements – The spatial arrangement of mechanically bonded components affording a distinction between mechanostereoisomers which can be converted by circumrotation, translation or rocking motions constrained by mechanical bonds; **Energy ratchet mechanism** – A mechanism by which directed motion and pumping is driven by external or light-driven modulation of both the depths of energy wells (relative state energies) and the heights of energy barriers (relative transition state energies); **Information ratchet mechanism** – Mechanism by which directed motion and pumping is controlled by modulation of energy barrier heights in selected states where allosteric feedback is used to determine in which states the energy barriers are raised and lowered. All chemically activated biomolecular motors and pumps driven by catalysis of an exergonic chemical reaction (ATP hydrolysis or ion transport) operate as information ratchets; **Mechanical bond** – An entanglement in space between two or more components such that they cannot be separated without breaking or grossly distorting chemical bonds; **Mechanostereochemistry** – The stereochemistry of molecules with mechanical bonds; **Molecular motor** – A molecule that interfaces chemical, electrochemical, and mechanical processes in a far-from-equilibrium environment. During their operation, molecular motors act as conduits that process energy, some of which is "siphoned off" in order to influence the trajectory of a local system, allowing it to move away from its inherent thermal equilibrium state; **Molecular pump** – A molecule that, when supplied with energy, transports ions or small molecules energetically uphill in a manner that is repetitive and progressive, creating concentration gradients; **Molecular shuttle** – A degenerate bistable rotaxane with two equivalent recognition sites for a ring that is able to dart back and forth between them; **Molecular switch** – A molecule that can be toggled reversibly between two or more equilibrium states by the application of a stimulus; **Pseudorotaxane** – A complex in which one linear molecule protrudes through the cavity of another ring-shaped molecule. The two components, which are held together by their mutual noncovalent bonding interactions, do not possess a mechanical bond; **Rotaxane** – A mechanically interlocked molecule consisting of (a) ring(s) encircling a dumbbell from which the ring(s) cannot escape on account of the bulky groups (stoppers) located at both ends of the dumbbell; **Thermodynamic nonequilibrium** – A situation in which the state probabilities of molecules in a system do not coincide with the energies according to a Boltzmann distribution.

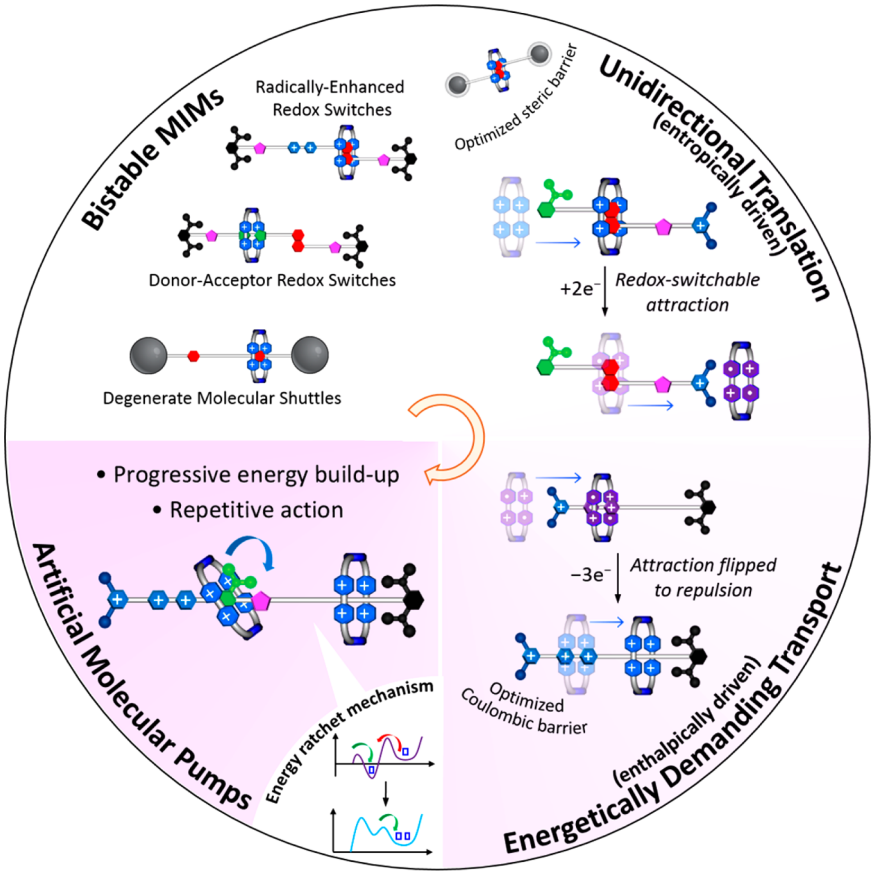

Figure 1. Evolution of donor−acceptor and radically enhanced MIMs from molecular shuttles and bistable switches to artificial molecular pumps. ***Upper left quadrant*****: redox-switchable bistable rotaxanes evolve from molecular shuttles.** ***Upper right quadrant*****: Relative unidirectional movement by the ring and rod components of a [2]pseudorotaxane.** ***Lower right quadrant*****: energetically demanding transport of a ring relative to a dumbbell involving radical−radical interactions.** ***Lower left quadrant*****: artificial molecular pumps driven repetitively and progressively.**

laws of thermodynamics. Rather, they capture some of this energy and use it to perform useful work, employing ratchet mechanisms[3,6,15] which, on account of periodic changes in kinetic barriers, do not necessarily proceed toward the global thermodynamic minimum.

This review (1) describes the recent developments that we have made in the design, synthesis, and operation of artificial molecular pumps that, when supplied with energy, create high energy MIMs as a result of ratchet-driven transport and (2) outlines a theoretical framework for linking the autonomous operation of the pumps to the catalysis of a chemical reaction. At the outset of this program of research, we challenged ourselves to use synthetically simple components with minimalistic design and to avoid the formation and cleavage of covalent bonds. Our progress toward this goal is summarized schematically in Figure 1, which outlines, in a clockwise fashion, starting in the upper-left quadrant and finishing in the bottom-left quadrant, the stages of (i) drawing inspiration from the recognition motifs present in bistable MIMs; (ii) identifying the means of controlling association and dissociation kinetics of the **CBPQT**$^{4+}$ ring with a constitutionally asymmetric substrate; (iii) capturing the ring as part of a high energy, kinetically stable entanglement with a molecular dumbbell, and (iv) assembling, optimizing, and operating an artificial molecular pump that runs repetitively and progressively to drive a system away from equilibrium.

A MOLECULAR PUMP PROTOTYPE

In its tetracationic form, **CBPQT**$^{4+}$ encapsulates π-electron rich substrates, such as DNP derivatives carrying oligoethylene glycol chains, by virtue of favorable [C−H···O] hydrogen bonds and donor−acceptor interactions with typical association constants (K_a) in MeCN solution in the region[43] of 10^3−10^4 M^{-1}. The ring, however, is redox active—a property which allows its recognition properties to be changed dramatically upon reduction to its dicationic bisradical form, namely, **CBPQT**$^{2(\bullet+)}$. Donor−acceptor noncovalent bonding interactions and [C−H···O] hydrogen bonding are weakened significantly in this reduced form and radical−radical pairing interactions predominate instead.[44,45] Consequently, we set out to take advantage of this redox-stimulated switching as a convenient way to control the thermodynamic energy minima in systems based upon **CBPQT**$^{4+}$. Inspired in

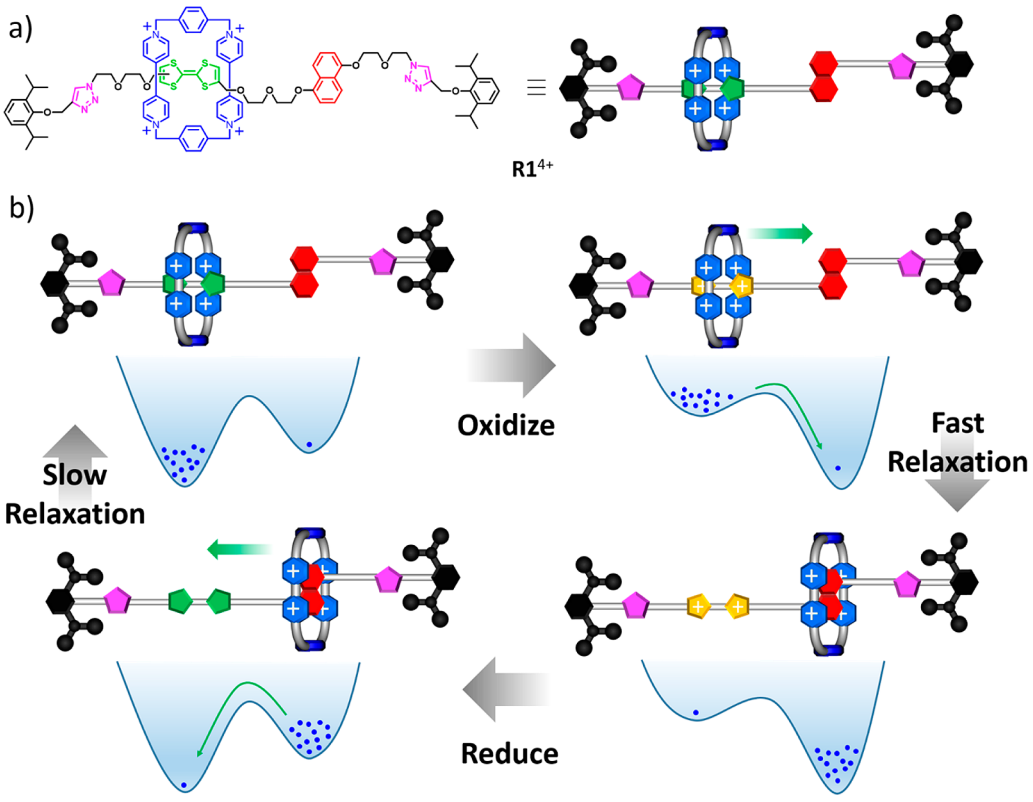

Figure 2. (a) Structural formula and graphical representation of the bistable [2]rotaxane R1^{4+}. Note that the CBPQT^{4+} ring (blue) prefers to encircle the TTF (green) rather than the DNP (red) unit by a factor of >9:1. (b) Redox-controlled operation of a molecular switch. When oxidation of the TTF unit occurs to give the TTF^{2+} dication (yellow), Coulombic repulsion results in the translation of the CBPQT^{4+} ring to the neutral DNP unit. (In fact, the CBPQT^{4+} ring moves as soon as the intermediate TTF$^{\bullet+}$ radical cation is formed.) This change in co-conformation is fast. When the TTF^{2+} dication is reduced back to the neutral TTF unit, the CBPQT^{4+} ring returns relatively slowly back to the TTF unit at the expense of thermal energy. In this manner, the switch is reset and no work is done. The number of balls in the wells represents the relative occupation probabilities.

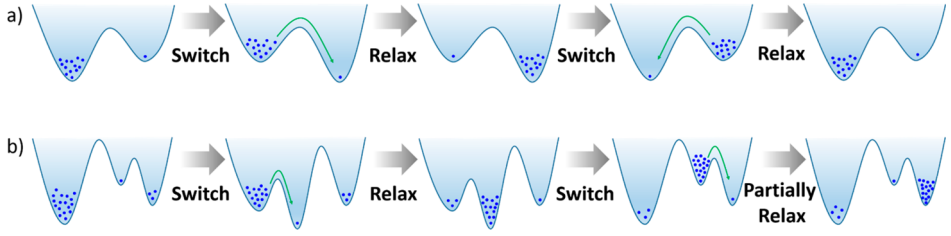

Figure 3. Energy profiles for (a) a molecular switch operating under thermodynamic control for most of the time and (b) a molecular machine operating under kinetic control overall with thermodynamically controlled steps. Here, the molecular machine is employing an energy ratchet mechanism wherein energy wells are raised and lowered in concert with energy barriers being lowered and raised. This mechanism requires the input of energy. We use the term "partially relax" since in the long-time limit the nonequilibrium probability distribution on the far right will inexorably relax to the equilibrium distribution on the far left. In the short-time situation, however, the nonequilibrium distribution can be harnessed to do work on the environment. This step is the essential one that turns a switch into a machine.

part by the contributions to the theory and formalisms of ratchet mechanisms,[3,4,15] as well as numerous elegant experimental demonstrations by Leigh,[6,7,46–49] and Credi[16,50,51] in the context of MIMs and supramolecules, respectively, we realized that developing additional elements of control over the kinetics of **CBPQT**$^{4+}$ association and dissociation would allow us to exploit (Figure 1) its recognition properties in the context of thermodynamic nonequilibrium systems. Given the highly charged and compact structure of **CBPQT**$^{4+}$, we anticipated that this kind of kinetic control might be achieved by introducing (Figure 4a) two complementary types of "barriers" as structural elements into **DB1**$^{+}$. On the one hand, neutral end groups whose size matches closely the dimensions of the **CBPQT**$^{4+}$ cavity should be able to influence the kinetics, by acting as "steric barriers",[52,53] while on the other hand, positively charged[54] "Coulombic barriers" are expected to impede the motion of the ring, based mainly on electrostatic repulsion. Importantly, the effect of this second type of barrier is subject to the oxidation state of the ring and is, consequently, stimulus-dependent.

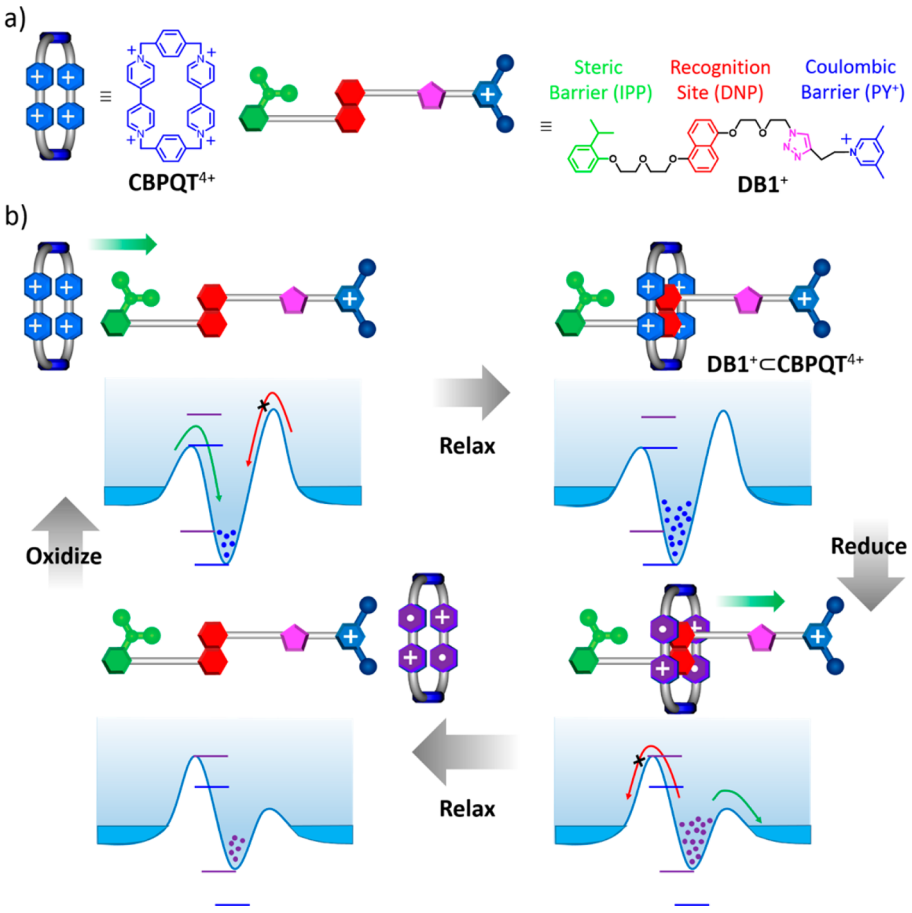

Figure 4. (a) Structural formulas and graphical representations of the CBPQT^{4+} ring and the dumbbell DB1^{+}. (b) Redox-controlled operation of a molecular pump prototype based on this ring and dumbbell which, at the onset, are separate species in solution. They form the 1:1 donor–acceptor complex DB1^{+}⊂CBPQT^{4+} as a result of the ring threading mechanostereoselectively onto the dumbbell over the neutral (green) IPP end group. Reduction of the CBPQT^{4+} ring to the bisradical dication (purple), namely, CBPQT$^{2(\bullet+)}$, impairs substantially the donor–acceptor stabilizing interaction with the DNP unit and leaves the reduced ring relatively free to leave the dumbbell by passing over the positively charged PY^{+} end group (blue) now that the electrostatic forces have been considerably diminished while the size of the cavity of the ring has decreased, raising the barrier to its departing by passing over the more bulky neutral IPP end group. Oxidation of the ring back to CPBQT^{4+} re-establishes the starting state where both the ring and the dumbbell reside in solution. Relative unidirectional motion has been achieved, but no work has been done. The blue and purple horizontal lines on the energy profiles beside the energy wells and barriers serve to indicate how they are raised and lowered during the redox cycle. The chemical potential of the ring in bulk solution is represented by the level of the dark blue "Fermi sea", and the probability distribution for the occupancy of the recognition site (energy well) is represented by the discrete number of balls present in the well.

In the first instance, we investigated[43] the rate of slippage of the **CBPQT**$^{4+}$ ring onto a series of constitutionally symmetric dumbbell-shaped molecules with neutral, size complementary groups at their termini and a DNP binding site located at their midriff. From a combined computational and experimental screen[43] of approximately 60 substituted neutral end groups, a handful were identified as potential steric barriers. A 2-isopropyphenyl (IPP) end group, for example, was found to slow down the association of the **CBPQT**$^{4+}$ ring with dumbbells to the minute time scale with activation energy barriers in the range of 15.4–16.9 kcal mol^{-1}. By employing a constitutionally asymmetric dumbbell **DB1**$^{+}$ with an IPP unit at one end and a 3,5-dimethylpyridinium (PY^{+}) Coulombic barrier at the other, we went on to demonstrate[55] that the dumbbell and ring undergo unidirectional motion relative to one another in response to redox cycling, *i.e.*, the ring threads onto the dumbbell from one end and dethreads from the other, as depicted in the upper right quadrant of Figure 1.

Stabilizing donor–acceptor charge transfer interactions between the DNP binding site at the center of **DB1**$^{+}$ and **CBPQT**$^{4+}$ favor (Figure 4b) the formation of the [2]pseudorotaxane **D1**$^{+}$⊂**CBPQT**$^{4+}$, which was observed in MeCN solution by UV–vis and ^{1}H NMR spectroscopies. By measuring the rate (1.6 ± 0.04 M^{-1} s^{-1}) of complex formation after mixing **DB1**$^{+}$ and **CBPQT**$^{4+}$ and by comparing it to the rates observed (5.7 ± 0.3 M^{-1} s^{-1} for IPP and (2.0 ± 0.2) × 10^{-4} M^{-1} s^{-1} for PY^{+}) for constitutionally symmetrical dumbbells as controls, it became apparent that the ring threads preferentially onto the dumbbell from the IPP end. Indeed, the tetracationic ring experiences high

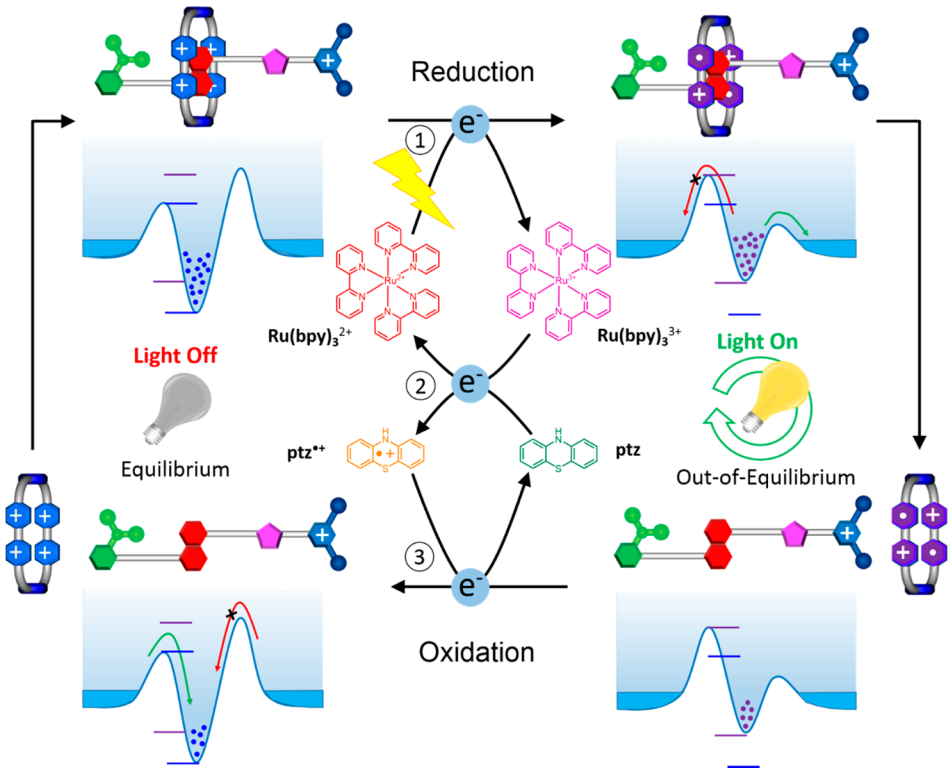

Figure 5. Molecular pump prototype powered by light, illustrated by means of a graphical representation of the mechanism of autonomous mechanostereoselective threading/dethreading of the [2]pseudorotaxane. Step ①: Reduction of the [2]pseudorotaxane by $Ru(bpy)_3^{2+}$ acting as a photosensitizer. Step ②: Back electron transfer to $Ru(bpy)_3^{3+}$ from the electron relay ptz. Step ③: Oxidation of the reduced $CBPQT^{2(\bullet+)}$ ring back to $CBPQT^{4+}$ by the $ptz^{\bullet+}$ radical cation. The operating efficiency is not so high.

Coulombic repulsion from the like-charged PY^+ end group, creating a relatively high kinetic barrier to threading of 22.9 kcal mol^{-1}, markedly larger than the 16.9 kcal mol^{-1} barrier to threading from the IPP end. The relative barrier heights are flipped (Figure 4b) when the ring is reduced to **CBPQT**$^{2(\bullet+)}$. The lower charge on the ring diminishes the repulsive electrostatic interactions, allowing the ring to traverse the PY^+ group more easily than it would the IPP terminus, *i.e.*, with a lower free energy of activation. Simultaneously, the donor–acceptor interactions are weakened, resulting in a net dethreading of the ring. Reduction of the ring was effected chemically by the addition of an excess of Zn dust, or electrochemically during cyclic voltammetry experiments. DFT calculations suggest[55] that the ring also contracts a little upon reduction, an observation which may heighten the effect of the steric barrier somewhat, even though this effect is relatively minor. The overall outcome is that **CBPQT**$^{4+}$ rings thread onto **DB1**$^+$ by passing the IPP barrier preferentially in order to form a [2]pseudorotaxane before the reduction step causes them to dethread over the PY^+ end. Thus, in a relative sense, the ring is transported from one side of the dumbbell to the other on account of changes that occur in energy maxima (barrier heights) and minima (binding interactions) as its redox state is altered. This oscillation in the magnitude of both kinetic energy barriers and energy wells amounts to what is known as an "energy ratchet" mechanism. The change in the heights of barriers and depths of wells occurs regardless of whether a well is occupied or not, *e.g.*, in the present case, the redox state of the viologen is altered by the applied stimulus whether or not it is part of an inclusion complex. Another alternative mechanistic pathway to access thermodynamic nonequilibrium states employs an "information ratchet", which exploits allosteric feedback to influence kinetic energy barriers. As a result, a system can move away from equilibrium without the depth of the energy wells ever having changed.[47] Biomolecular motors and pumps, driven by ATP hydrolysis (*e.g.*, kinesin and myosin) or proton transport across a membrane (*e.g.*, F1 ATPase and bacterial flagellar motors) function as information ratchets, where allosteric interactions switch the specificity of the molecular motor for reactant and product depending on the mechanical state of the motor. We will examine this mechanism in greater detail in the penultimate section of this review.

With appropriate experimental design, the redox cycle can be powered autonomously using light,[56] avoiding the generation of byproducts that accompany chemical reduction and oxidation[55] and also circumventing the constraints of microscopic reversibility. See Figure 5. With the use of **Ru(bpy)**$_3^{2+}$ as a

photosensitizer, phenothiazine (**ptz**) as an electron relay, and irradiating with 450 nm light, a photo redox reaction occurs in which electrons are transferred transiently from the **Ru(bpy)$_3$**$^{2+}$ to the ring, resulting in its reduction. Back transfer of electrons to the **Ru(bpy)$_3$**$^{3+}$ that is generated is delayed by its reversible reaction with **ptz**.[57] The resulting **ptz**$^{\bullet+}$ radical cation has a relatively long lifetime, allowing the reduced [2]pseudorotaxane the opportunity to dissociate before its ring component is eventually reoxidized. A steady state distribution is established during irradiation with a lower proportion of [2]pseudorotaxane than that present at thermal equilibrium.[3] In the act of dissipating the light energy that is absorbed during irradiation, the system moves away from thermal equilibrium. When the irradiation is stopped, equilibrium is gradually reestablished over a period of several minutes.

While this prototypical system, based on **DB1**$^{+}$ and **CBPQT**$^{4+}$, demonstrates ratchet-driven translational motion, the ring returns to the bulk solution after traversing the thread. In other words, the product of one cycle is the same as its starting materials and no work is done. Moreover, the driving force for dissociation in the case of **D1**$^{+}\subset$**CBPQT**$^{2(\bullet+)}$ is largely entropic. Although stabilizing donor–acceptor interactions are diminished upon reduction, there is nevertheless some degree of attractive interaction[55] that remains. We were led, therefore, to consider the possibility that it may be beneficial to introduce an enthalpic driving force in both oxidation states, first of all to attract a ring, and then to repel it.

ENERGETICALLY DEMANDING TRANSPORT

By employing a *N*,*N*′-dialkyl-4,4′-bipyridinium (BIPY^{2+}) radical recognition site[44,45] in place of the DNP unit, we anticipated that we would be able to flip the interaction between the dumbbell and the ring back and forth from attraction to repulsion.[58] Somewhat counterintuitively, the reduced ring **CBPQT**$^{2(\bullet+)}$ has[45] a strong affinity for reduced BIPY$^{\bullet+}$ substrates with typical association constants, K_a, in the region of 10^4 M^{-1} in MeCN, forming a trisradical inclusion complex on account of pimerization[59,60] which occurs between the three radical cations. An enthalpic driving force for the components to separate from one another arises[58] after oxidation of the BIPY$^{\bullet+}\subset$**CBPQT**$^{2(\bullet+)}$ complex to BIPY$^{2+}\subset$**CBPQT**$^{4+}$ as a consequence of the repulsive electrostatic interaction between the tetracationic ring and the dicationic BIPY^{2+} site. Initially, in a thought experiment, we designed a radical–radical interaction-based hypothetical molecular pump prototype (Figure 6) where the DNP unit in the donor–acceptor system was replaced by a BIPY^{2+} unit. In this hypothetical prototype, we would expect the **CBPQT**$^{2(\bullet+)}$ ring to be attracted onto the BIPY$^{\bullet+}$ radical recognition site by passing over the PY^{+} end group

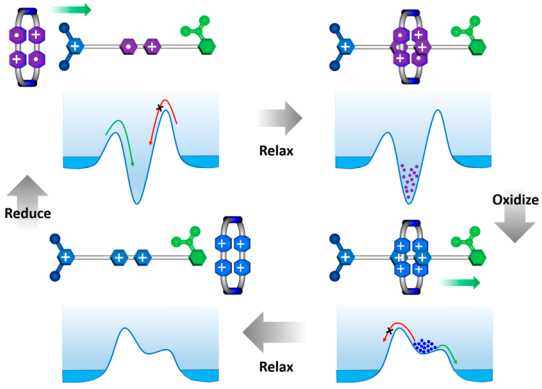

Figure 6. Graphical representations and energy profiles for a hypothetical molecular pump prototype based on radical–radical stabilizing interactions. In this hypothetical prototype, the formation of a strong 1:1 complex between a bipyridinium radical cation (BIPY$^{\bullet+}$) in a dumbbell with the same charged (PY^{+}) and neutral (IPP) end groups as before in the donor–acceptor based molecular pump prototype and the CBPQT$^{2(\bullet+)}$ bisradical dication causes threading of the ring to occur *via* the PY^{+} end. On oxidation, a push-button molecular switch is created by the generation of six positive charges where there were only three that were suppressed previously by radical–radical interactions. The net result is the generation of a considerable amount of potential energy that forces the CBPQT^{4+} ring to depart from the neutral IPP end group of the tricationic dumbbell. The cycle is completed on reduction of the ring and the dumbbell. Once again, relative unidirectional motion has been achieved, but no work is done.

under reducing conditions aided and abetted by strong 1:1 trisradical complex formation. On oxidation, we would expect the **CBPQT**$^{4+}$ ring to be pumped back into solution over the IPP end group on account of the Coulombic repulsion generated by the six positive charges. The hypothetical molecular pump prototype, however, is not easy to test experimentally. To ascertain if this hypothetical prototype might be applicable to the construction of an artificial molecular pump, we designed (Figure 7a) and synthesized[61] a homologous series of dumbbells **DB2**$^{3+}$–**DB6**$^{3+}$.

In each case, one end of the dumbbells **DB2**$^{3+}$–**DB6**$^{3+}$ is terminated by the same Coulombic barrier, PY^{+}, which is connected to a BIPY^{2+} recognition site by a short oligomethylene chain, Linker A. A longer oligoethylene glycol (**DB2**$^{3+}$) or oligomethylene (**DB3**$^{3+}$–**DB6**$^{3+}$) chain, connected to the other side of the BIPY^{2+} unit, is terminated by a bulky stopper. We anticipated that, if the combination of the Coulombic barrier and radical recognition site, namely, BIPY$^{\bullet+}$, attracts **CBPQT**$^{2(\bullet+)}$ rings under reducing conditions and then repels them in a relative unidirectional manner upon oxidation, the rings will become ensnared on this long, ring-collecting chain. See Figure 8. Their dissociation from the dumbbell will be opposed by the Coulombic barrier on one end and the bulky stopper on the other, trapping the dumbbell and ring component together kinetically in a high-energy state that lacks any significant stabilizing interactions between the dumbbell and ring components.[62,63] Whether the

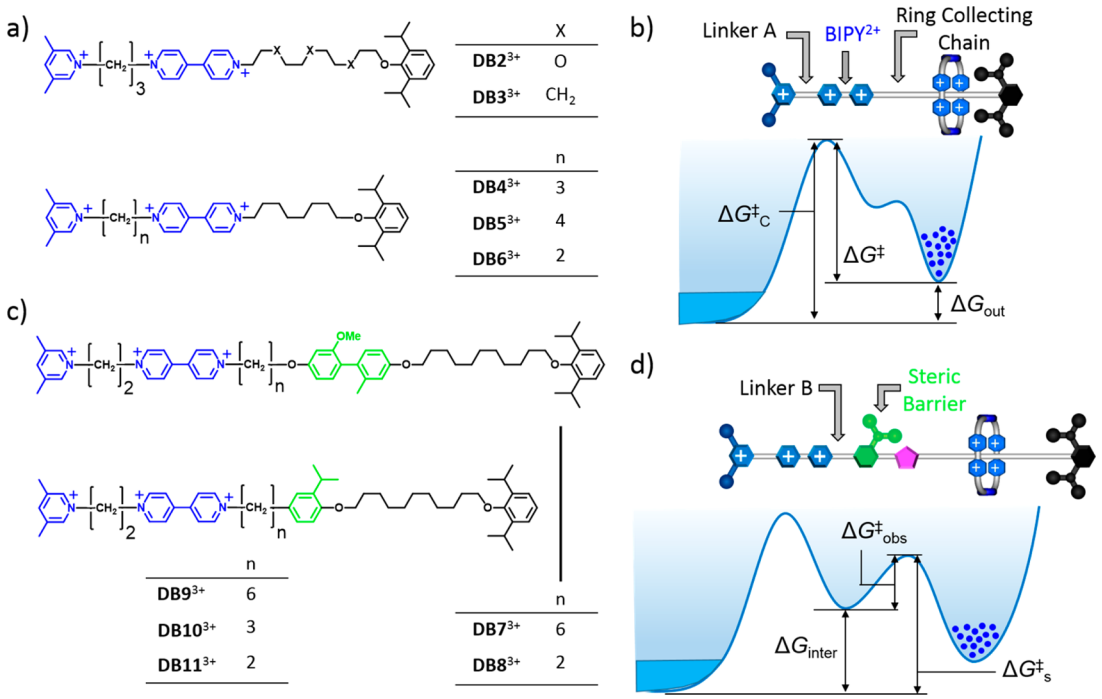

Figure 7. Structural formulas of dumbbells $DB2^{3+}$–$DB11^{3+}$ and graphical representations and the energy profiles of corresponding dumbbells with $CBPQT^{4+}$ rings on them. The positive charges on the dumbbells discussed in this review are all balanced by PF_6^- anions. (a) Structural formulas of the dumbbells $DB2^{3+}$–$DB6^{3+}$ employed in the ring-collecting chain and Coulombic barrier optimization experiments. (b) Graphical representations and energy profiles of corresponding dumbbells with a $CBPQT^{4+}$ ring on them. Coulombic barrier $\Delta G^{\ddagger}_{C}$ optimization was achieved by varying linker A. The height of $\Delta G^{\ddagger}_{C}$ changes when the length of liner A changes. (c) Structural formulas of the dumbbells $DB7^{3+}$–$DB11^{3+}$ employed in the steric barrier optimization experiments. (d) Graphical representations and energy profiles of corresponding dumbbells with a $CBPQT^{4+}$ ring on them. The observed steric barrier $\Delta G^{\ddagger}_{obs}$ optimization was achieved by varying linker B. The height of $\Delta G^{\ddagger}_{obs}$ changes when the length of linker B changes. For a detailed explanation of the free energy profiles in (b) and (d), see the text.

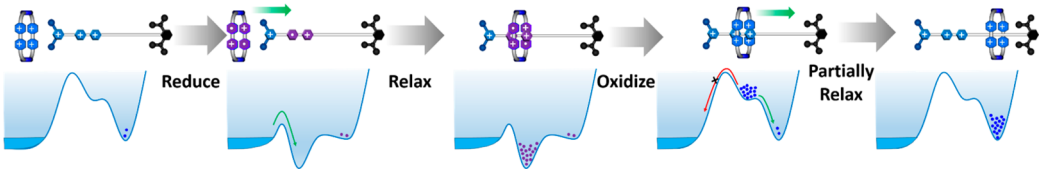

Figure 8. Graphical representations and energy profiles for the operation of a simplified artificial molecular pump. In this simplified artificial molecular pump, the $CBPQT^{4+}$ ring and the dumbbell repel each other initially because of Coulombic repulsion. On reduction, the Coulombic barrier drops dramatically as the positive charge number on the ring falls. The formation of a strong 1:1 complex between a bipyridinium radical cation ($BIPY^{\bullet+}$) in the dumbbell and the $CBPQT^{2(\bullet+)}$ bisradical dication attracts the ring onto the $BIPY^{\bullet+}$ unit *via* the PY^+ end. On oxidation, the strong Coulombic repulsion generated by six positive charges pumps the $CBPQT^{4+}$ ring onto the ring-collecting chain since the high Coulombic barrier from PY^+ end group is restored. The net result is that, in a redox cycle, a $CBPQT^{4+}$ ring is transported from bulk solution phase to a ring-collecting chain. Note that there is no/little binding interaction between the $CBPQT^{4+}$ ring and the ring-collecting chain, since the ring is forced onto the chain by redox chemical energy. Work is done.

product would be classified as a [2]pseudorotaxane or a [2]rotaxane would depend[64] upon its kinetically stability, *i.e.*, whether the ring could eventually overcome the kinetic barrier to dethreading on a measurable time scale. Given this design, "work" would be performed in the sense that an energetically demanding state—the metastable [2]pseudorotaxane or high-energy [2]rotaxane—would be obtained after a redox cycle, even though each of the individual dumbbell and ring components are returned to their initial oxidation states.

In practice, equimolar mixtures of the dumbbell component and ring were reduced together in CD_3CN solution by stirring with an excess of Zn dust. After filtering to remove the heterogeneous reducing agent, the solutions were oxidized with either tris(4-bromophenyl)aminium hexachloridoantimonate or $NOPF_6$, before analyzing them by ^1H NMR spectroscopy. We demonstrated[61] that dumbbells **$DB2^{3+}$**–**$DB5^{3+}$** were capable of capturing a **$CBPQT^{4+}$** ring during this chemical redox cycle, acting as rudimentary artificial molecular pumps. There was significant variation in the efficiency of the pumping process and the kinetic stability of the product for each dumbbell, however, which led us toward an optimized system. It transpired that a ring-collecting oligomethylene chain is preferable

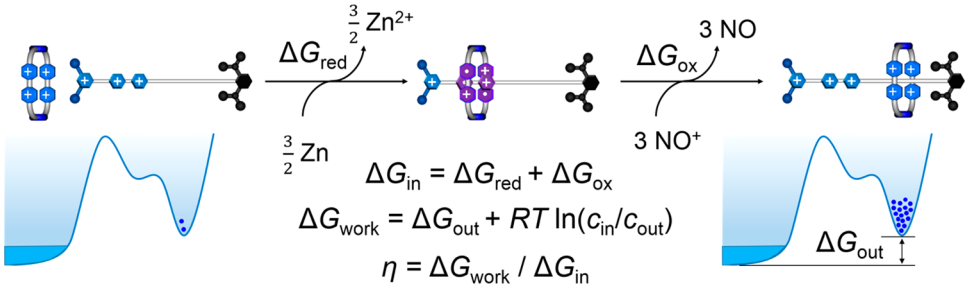

Figure 9. Graphical representations and energy profiles for a simplified artificial molecular pump and redox chemistry involved in the operation process. For each dumbbell and CBPQT^{4+} ring, the redox process involves the transfer of three electrons, provided by the reducing reagent Zn and oxidation reagent NO^{+}. The value of ΔG_{in} is the total energy input that comes from the free energy changes of the reducing reagent ΔG_{red} and the oxidizing reagent ΔG_{ox}. The work done ΔG_{work} comes from the CBPQT^{4+} energy difference ΔG_{out} and the increase in the effective concentration when rings are restrained on the ring-collecting chain compared with when they are free in solution. The energy conversion efficiency η is defined as the ratio of work done to the total energy input. See text for a detail explanation of the equations.

to an oligoethylene glycol chain. A comparison of **DB2**$^{3+}$ and **DB3**$^{3+}$ revealed that the presence of an oligoethylene glycol chain leads to faster dissociation of the entangled ring and dumbbell. The transition state to dethreading, in which the ring approaches the Coulombic barrier, appears[43,61] to be stabilized somewhat by [C−H···O] hydrogen bonding interactions between **DB2**$^{3+}$ and **CBPQT**$^{4+}$. For the purposes of optimizing the system to operate in MeCN, therefore, oligoethylene glycol chains were discounted. It should be noted, however, that the importance of these hydrogen bonding interactions is diminished in aqueous solution, where an oligoethylene glycol dumbbell and the chloride counterions might be better choices.

Upon changing the length of Linker A, which connects the PY^{+} unit and BIPY^{2+} units, we found (Figure 7b) that variation by just one methylene group can have a dramatic influence[61] on the effectiveness of the Coulombic barrier, $\Delta G^{\ddagger}_{C}$. A propylene linker (**DB4**$^{3+}$) results in a system in which the $\Delta G^{\ddagger}_{C}$ barrier is able to prevent the **CBPQT**$^{4+}$ ring from dethreading at room temperature but not high enough to keep the ring on the chain when heating. Surprisingly, when the linker is elongated to butylene (**DB5**$^{3+}$), the $\Delta G^{\ddagger}_{C}$ barrier becomes too low to prevent the oxidized ring and dumbbell from dissociating even at low temperature. No trace of **D5**$^{+}$⊂**CBPQT**$^{4+}$ was detected by ^{1}H NMR spectroscopy after a chemical redox cycle. Conversely, when a bismethylene linker (**DB6**$^{3+}$) separates the PY^{+} and BIPY^{2+} units, the $\Delta G^{\ddagger}_{C}$ barrier is so high that the resulting threaded product is stable in refluxing acetonitrile! A full analysis based on the dissociation kinetics of **CBPQT**$^{4+}$ from the series of dumbbells revealed that, empirically, the addition or removal of one methylene group from Linker A changes the barrier to dissociation by approximately 7 kcal mol^{-1}. DFT calculations[61] provided further insight into the reason behind this remarkably sensitive relationship between structure and function. It appears that the potential energy surface, created as **CBPQT**$^{4+}$ and **DB5**$^{3+}$ dissociate from one another, features two separate maxima, corresponding to BIPY^{2+}⊂**CBPQT**$^{4+}$ and PY^{+}⊂**CBPQT**$^{4+}$ transition states, neither of which are particularly high in energy. By contrast, a single, much higher peak was predicted by calculation for **DB6**$^{3+}$. The proximity of the charged BIPY^{2+} and PY^{+} groups, enforced by the short bismethylene linker, causes them to act in unison, presenting one insurmountable Coulombic barrier to the ring. In the subsequent design of artificial molecular pumps, therefore, a bismethylene linker was used to ensure that the Coulombic barrier is sufficiently large to act essentially as a one-way valve, preventing an already threaded **CBPQT**$^{4+}$ ring from returning to the bulk solution.

Aside from Linker A, the length of the ring-collecting chain also plays a role in determining the energetics of the system. By comparing the behavior of **DB3**$^{3+}$ with that of **DB4**$^{3+}$, we discovered, as might be anticipated, that a longer ring-collecting chain leads to a more kinetically stable (pseudo)rotaxane. A shorter chain imposes more stringent restrictions upon the conformational freedom of both the ring and dumbbell components, as well as holding the positively charged groups in closer proximity. The result is that **DB4**$^{3+}$⊂**CBPQT**$^{4+}$ lies in a higher energy state (larger ΔG_{out}) than its **DB3**$^{3+}$-derived homologue and, consequently, requires a lower energy of activation $\Delta G^{\ddagger}$ to surmount the Coulombic barrier.

As the molecular pumps are powered by chemical reduction and oxidation, employing reagents with known redox potentials, the total energy input ΔG_{in} can be calculated to be about 140 kcal mol^{-1} by summing ΔG_{red} and ΔG_{ox}, based upon the redox potentials of the Zn^{2+}/Zn and NO^{+}/NO couples. The energy output ΔG_{out}, on the other hand, can be estimated (Figure 9) to be 7−14 kcal mol^{-1} based upon the experimentally determined thermodynamic parameters and the results of DFT calculations.[61] To estimate the total work ΔG_{work} that is performed in the process of entrapping a ring on the dumbbell, one must also take into account (Figure 9) the increase in effective concentration that occurs when a **CBPQT**$^{4+}$ ring is

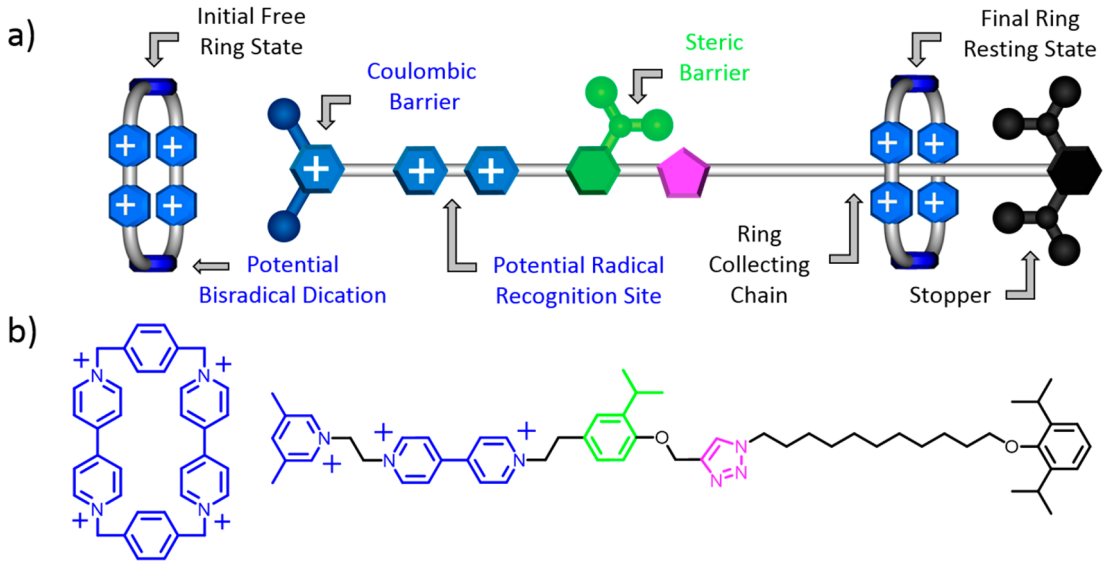

Figure 10. (a) Graphical representation of the ring and dumbbell components of an artificial molecular pump. (b) Structural formulas of these two components.

trapped on the ring-collecting chain in addition to the energy output ΔG_{out}. With the use of an approximation where the trapped ring is held within a 1 nm^3 space by the constraints of the dumbbell, its effective concentration on the ring-collecting chain is roughly equivalent to 1.7 M. The solution phase concentration we employ is 1 mM. The work done in confining the ring, $RT \ln(c_{in}/c_{out})$, where c_{in} is the effective concentration of **CBPQT**$^{4+}$ trapped on ring collecting chain and c_{out} is the concentration of the free ring in bulk solution, is about 4.4 kcal mol^{-1}. Energy conversion efficiencies, η, which measure (Figure 9) the proportion of the energy input that is transferred to the (pseudo)rotaxane, are found to be about 8−13% for this system.

PERFORMING WORK REPETITIVELY

The optimization[65] of the molecular pump's structure from a drawing on paper to real chemistry in the laboratory has been painstakingly carried out (Figure 10) in a step-by-step manner.[66] While the optimal structural elements of Nature's molecular motors have emerged during millennia of natural selection, clearly a more rational and directed approach must be taken in order to optimize design parameters of artificial molecular pumps.

To reach a rational understanding of the steric barriers, we synthesized[66] **DB7**$^{3+}$ with a potential steric barrier (Figure 7c) in the form of a disubstituted biphenyl derivative incorporated in its midriff between the radical recognition unit and ring collecting chain. When **DB7**$^{3+}$ and the **CBPQT**$^{4+}$ ring are reduced and then oxidized, the ^{1}H NMR spectrum shows that the **CBPQT**$^{4+}$ ring is located beside the phenylene ring carrying the methoxy group before rearranging slowly to the phenylene ring with the methyl substituent, but not continuing further to reside on the oligomethylene chain on account of apparent donor−acceptor interactions between the steric barrier and the ring. When a second redox cycle with excess of **CBPQT**$^{4+}$ is performed, a second **CBPQT**$^{4+}$ ring locates itself beside the phenylene ring carrying a methoxy group, forcing the first **CBPQT**$^{4+}$ ring onto the oligomethylene chain while the second **CBPQT**$^{4+}$ ring rearranges slowly onto the phenylene ring with the methyl substituent. The formation of the donor−acceptor complex between the **CBPQT**$^{4+}$ ring and steric barrier was unexpected. **DB8**$^{3+}$ with the shorter (n = 2) linker between the charged BIPY^{2+} unit and the steric barrier was also synthesized and subjected to redox cycling in the presence of **CBPQT**$^{4+}$. While we might expect that the increased Coulombic repulsion would destabilize the donor−acceptor complex, it fails to do so. Although the performance of the molecular pump, containing the disubstituted biphenyl unit as a speed bump, proved that we can pump a second ring, the ring, rather unfortunately, also forms a donor−acceptor complex with the biphenyl unit. The unexpected noncovalent bonding interaction calls into question the concept of moving rings energetically uphill.[67,68]

We decided to return to employing the IPP unit[66] as the speed bump. Surprisingly, however, the observed (Figure 7d) steric barrier, $\Delta G^{\ddagger}_{obs}$, was too high for the ring to pass over the IPP unit in **DB9**$^{3+}$, underscoring yet again that, although a qualitative estimate of pump performance can be made at the design stage, the delicate balance of the energetics is far from easy to predict quantitatively, even when drawing comparisons with analogous compounds. We found, however, that this situation could be turned to our advantage. Even though any structural alterations to the steric barrier will result in significant changes[43] in $\Delta G^{\ddagger}_{S}$, we knew[55] that the IPP unit did not act as a stopper for the

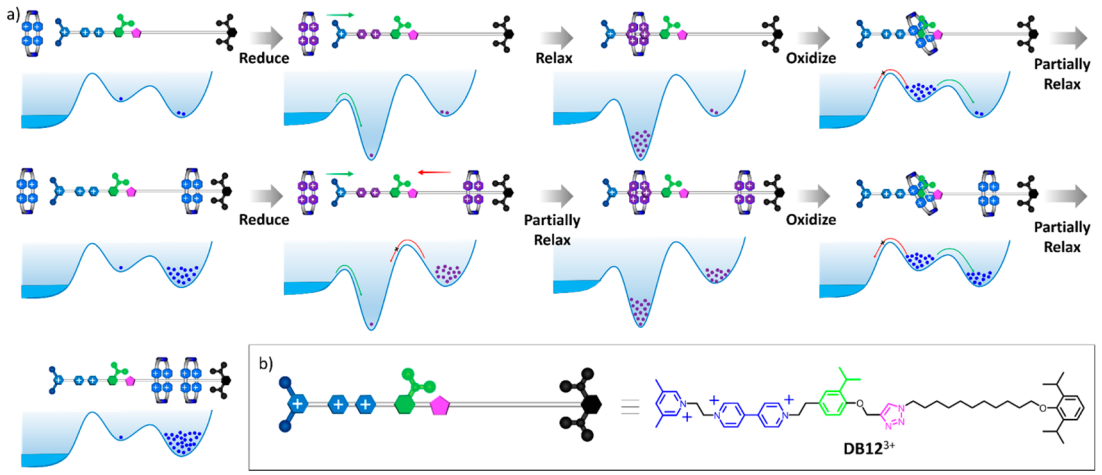

Figure 11. (a) Graphical representations and energy profiles for the operation of an artificial molecular pump. The CBPQT^{4+} ring and the dumbbell repel each other initially because of Coulombic repulsion. On reduction, the Coulombic barrier drops dramatically as the positive charge on the ring diminishes. The formation of a strong 1:1 complex between the bipyridinium radical cation (BIPY$^{\bullet+}$) in the dumbbell and the CBPQT$^{2(\bullet+)}$ bisradical dication attracts the ring onto the BIPY$^{\bullet+}$ unit *via* the PY^{+} end. On oxidation, strong Coulombic repulsion generated from six positive charges forces the CBPQT^{4+} ring to pass over the neutral IPP unit since the high Coulombic barrier from the PY^{+} end group is restored. When a second reduction is performed, the first CBPQT$^{2(\bullet+)}$ ring trapped on the ring-collecting chain cannot return to occupy the BIPY$^{\bullet+}$ radical recognition site because of steric hindrance from the IPP unit. A second CBPQT$^{2(\bullet+)}$ ring can be attracted from solution and pumped onto the ring-collecting chain after being back to the fully charged state. The net result is that in two redox cycles, two CBPQT^{4+} rings are transported from bulk solution phase to a ring-collecting chain. Since there is no/little binding interaction between the CBPQT^{4+} rings and the ring-collecting chain, the rings are forced onto the chain by redox chemical energy one by one. Work is done repetitively and progressively. (b) Structural formula and graphical representation of DB12^{3+}.

CBPQT^{4+} ring in the **DB1**$^{+}$ system. An alternative way of decreasing $\Delta G^{\ddagger}_{obs}$ is to increase the free energy, ΔG_{inter}, of the intermediate, while retaining the IPP unit as the steric barrier. Hence, **DB10**$^{3+}$ with its shorter linker between the BIPY^{2+} and IPP units was prepared. The ΔG_{inter} value in the case of **DB10**$^{3+}$ is higher than that of **DB9**$^{3+}$ since the **CBPQT**$^{4+}$ ring in the former is closer to the liked-charged BIPY^{2+} unit when located on the IPP unit after each redox cycle. As we expected, the **CBPQT**$^{4+}$ ring can pass over the IPP unit completely during a few hours on heating at 60 °C with an observed activation energy barrier, $\Delta G^{\ddagger}_{obs}$, of 26 kcal mol^{-1}. Further shortening of the linker in **DB11**$^{3+}$ to that of a bismethylene unit results in a decrease of the $\Delta G^{\ddagger}_{obs}$ value to 23 kcal mol^{-1}, allowing the rearrangement to take place at 40 °C, a temperature which proved to be ideal in our further investigations.

A FULLY FUNCTIONAL ARTIFICIAL MOLECULAR PUMP

Having optimized all the structural parameters, we produced[66] a molecular pump (Figure 3b) with all the predetermined structural features and a terminal triple bond with modularity to aid and abet further synthesis. The pumping unit was connected to an oligomethylene, ring-collecting chain using a copper-catalyzed azide−alkyne cycloaddition. When the resulting artificial molecular pump **DB12**$^{3+}$ was tested, it behaved (Figure 11) in the manner expected of it.

When an excess of **CBPQT**$^{4+}$ in the presence of **DB12**$^{3+}$ was reduced with activated Zn dust in CD_3CN, the reaction mixture acquired a characteristic purple color within seconds, indicating the formation of a trisradical tricationic complex. After filtering off the Zn dust, $NOPF_6$ was added to the filtrate and the purple solution returned immediately to being a light yellow color. The co-conformational rearrangement, wherein the **CBPQT**$^{4+}$ ring passes slowly over the IPP unit and is trapped on the ring-collecting chain, was monitored by ^{1}H NMR spectroscopy. The redox process was repeated through another cycle in order to trap a second **CBPQT**$^{4+}$ ring on the ring-collecting oligomethylene chain. From the kinetic data obtained by analysis of the ^{1}H NMR spectra recording the two co-conformational rearrangements, we estimated the yields of the [2]- and [3]rotaxanes to be 90 and 85%, respectively, with $\Delta G^{\ddagger}_{obs}$ values of 23.0 and 23.1 kcal mol^{-1}. These near-identical $\Delta G^{\ddagger}_{obs}$ values indicate that the two co-conformational rearrangements are independent processes where the trapping of the second **CBPQT**$^{4+}$ ring is not influenced by the presence of the first ring. On the basis of these findings, we are confident that the pumping unit can be made to function repetitively and progressively,[69] in order to trap multiple rings away from equilibrium, thus creating a concentration gradient in an artificial system.[70−73]

TOWARD AUTONOMOUS CHEMICALLY DRIVEN MOLECULAR PUMPS

The molecular motors illustrated in Figures 7−11 function as energy ratchets, where external modulation of both the well depths and barrier heights provides the energy to drive the system out-of-equilibrium, maintaining a much higher steady state probability of having

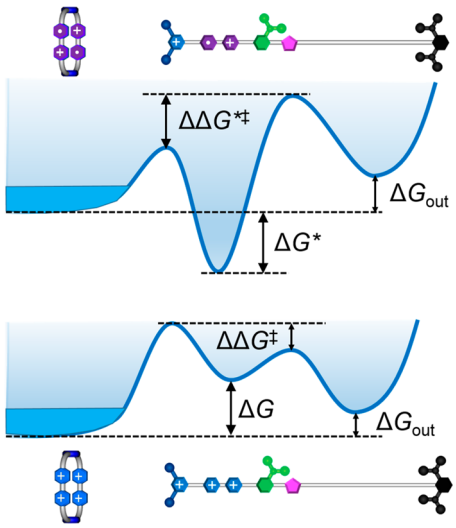

Figure 12. Graphical representations and energy profiles of an artificial molecular pump corresponding to both the reduced (top) and oxidized (bottom) states, as experienced by the CBPQT$^{2(\bullet+)}$/CBPQT^{4+} rings as a function of their positions along the dumbbell. The relative likelihood for a ring at the recognition site going to the ring-collecting chain *versus* the bulk solution is governed solely by the difference in barrier heights, $\Delta\Delta G^{\ddagger}$ and $\Delta\Delta G^{*\ddagger}$, in the oxidized and reduced forms, respectively.

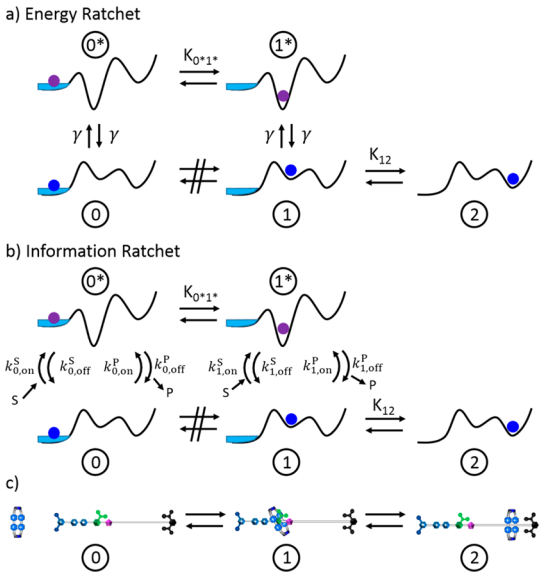

Figure 13. Energy profiles of the states (0, 0*, 1, 1*, and 2) of an artificial molecular pump operating under (a) an energy ratchet mechanism and (b) an information ratchet mechanism along with (c) the corresponding graphical representations of the structural formulas for states 0, 1, and 2. Note that for easier comparison, we take the external switching for the energy ratchet to be governed by a rate process with rate constant γ, and where, instead of distributions, we focus on paths through the states. If $|\Delta\Delta G^{\ddagger}| \gg 0$, the direct transition 0 ⇌ 1 is effectively blocked and the relative state probabilities of states 2 and 0 at steady state can be calculated as the ratio of the product of the total transition rates from 0 to 2 divided by the product of the total transition rates from 2 to 0. The seemingly small but enormously important differences between the recipes for the energy ratchet and the information ratchet are that there are two pathways between 0 and 0* and between 1 and 1* in the information ratchet, and that the forward and reverse rate constants for each pathway in the information ratchet obeys microscopic reversibility—their ratio is proportional to the energy difference between the two states they connect—and the forward and reverse transition constants for the energy ratchet do not obey microscopic reversibility.

rings encircling oligomethylene chains than is the case at thermodynamic equilibrium. The energy profiles of the integrated system that correspond to both the oxidized and reduced states are shown in Figure 12. Operation of the pumps is achieved by cycling between redox states, as we have demonstrated experimentally using chemical reagents, *e.g.*, Zn and $NOPF_6$. A key consideration for the discussion that follows, however, is that it is necessary to add these reagents in sequence in order to oscillate between the potential energy surfaces. It follows that the machine is not "autonomous". It relies on external intervention at each step in order to work. While we have also demonstrated (Figure 5) that the introduction of a photosensitizer can interface a similar energy ratchet with an autonomous, photochemically driven redox process, Nature has evolved an entirely different strategy to impart autonomy to its chemically fueled machines.

In contrast with artificial molecular pumps, chemically driven biomolecular motors and pumps, such as kinesin,[74] myosin[75] (muscle), F1 ATPase,[76] and the bacterial flagellar motor,[77] work as information ratchets.[78,79] They are catalysts (enzymes) for an exergonic chemical reaction and their operation hinges upon changes in the specificity of the molecular motor for the substrates and products of this driving reaction as a function of the mechanical state of the motor. To contrast these two possibilities, consider Figure 13, where we have presented the energy ratchet (Figure 13a), with a Poisson distributed time constant, γ, for external switching between redox potentials to simulate switching driven by an internal process,[80] and information ratchet (Figure 13b) mechanisms. At first glance, these mechanisms seem very similar. The energy profiles governing the motions of the rings along the dumbbells are identical in the two mechanisms. It seems that we should be able to incant words like "binding of substrate deposits chemical energy to cause transition from one energy profile to the other" in order to explain how a chemical reaction (S ⇌ P) allows the optimized pump (Figure 10) to function as an energy ratchet. When we view the mechanisms through the lens of microscopic reversibility, however, we see that it is simply not the case.

If the energy difference between the two barrier heights, $\Delta\Delta G^{\ddagger}$, is large, the transitions shown as blocked in Figure 13 can be ignored and the stationary ratio between states can be easily calculated as the product of the net transitions rates between the states.

For the energy ratchet (Figure 13a), this calculation, based on eq1, is very simple:

$$\left(\frac{P_2}{P_0}\right)_{\text{energyratchet}} = K_{0^*1^*}K_{12} = e^{\Delta G - \Delta G^*}e^{-\Delta G_{\text{out}}} \quad (1)$$

where all energies are expressed in units of the thermal energy k_BT. If $\Delta G - \Delta G^* > 0$, the nonequilibrium fluctuations maintain the system in a nonequilibrium stationary state, in which the occupancy of the ring on the oligomethylene chain is greater than it would be at equilibrium. Moreover, if $\Delta G - \Delta G^* > \Delta G_{\text{out}}$, the nonequilibrium fluctuations maintain the system in a state where most of the ring-collecting chains are, on average, occupied with at least one ring, while continuous pumping can load several rings onto each dumbbell since the barrier between the recognition site and collecting chain is low only when the recognition site is occupied. When the recognition site is occupied, the ring on the collecting chain cannot go backward. This strategy was employed by Leigh[81] in designing a system that supports unidirectional rotation in a catenated system.

In an autonomous, chemically driven pump or motor, energy is provided by catalysis of an exergonic chemical reaction (*e.g.*, ATP hydrolysis or transport of ions across a membrane) rather than by light or by an external modulation of the thermodynamic parameters such as pH or redox potential. Consider the theoretical case where the ring catalyzes a reaction S⇄P by a Michaelis–Menten mechanism. Binding of substrate and release of product provide a mechanism for switching between two energy profiles. At first glance, the information ratchet appears to be very similar to the energy ratchet. On closer examination, however, there is a huge difference between the two: the rate constants must obey microscopic reversibility. The constraints of microscopic reversibility can be summarized in eq2 as

$$\frac{k^{\text{S}}_{0,\text{on}}k^{\text{P}}_{0,\text{off}}}{k^{\text{P}}_{0,\text{on}}k^{\text{S}}_{0,\text{off}}} = \frac{k^{\text{S}}_{1,\text{on}}k^{\text{P}}_{1,\text{off}}}{k^{\text{P}}_{1,\text{on}}k^{\text{S}}_{1,\text{off}}} = e^{\Delta\mu} \quad (2)$$

where $\Delta\mu = \mu_{\text{S}} - \mu_{\text{P}}$ is the chemical potential difference between substrate and product that drives the reaction. We also have a second constraint of microscopic reversibility obtained by recognizing (see eq 3) that the energy is a state function

$$\frac{k^{\text{S}}_{0,\text{on}}k^{\text{S}}_{1,\text{off}}}{k^{\text{S}}_{1,\text{on}}k^{\text{S}}_{1,\text{off}}} = \frac{k^{\text{P}}_{0,\text{on}}k^{\text{P}}_{1,\text{off}}}{k^{\text{P}}_{1,\text{on}}k^{\text{P}}_{0,\text{on}}} = e^{-(\Delta G - \Delta G^*)} \quad (3)$$

with these constraints, the ratio (P_2/P_0) can be calculated according to eq4 as the ratio of the products of the total rates from each state to be

$$\left(\frac{P_2}{P_0}\right)_{\text{informationratchet}} = \frac{(k^{\text{S}}_{0,\text{on}} + k^{\text{P}}_{0,\text{on}})(k^{\text{S}}_{1,\text{off}} + k^{\text{P}}_{1,\text{off}})}{(k^{\text{S}}_{0,\text{off}} + k^{\text{P}}_{0,\text{off}})(k^{\text{S}}_{1,\text{on}} + k^{\text{P}}_{1,\text{on}})}K_{0^*1^*}K_{12}$$
$$= \frac{(1 + s_0e^{\Delta\mu})(1 + s_1)}{(1 + s_0)(1 + s_1e^{\Delta\mu})}e^{-\Delta G_{\text{out}}} \quad (4)$$

where the constraints of microscopic reversibility were used to derive the second equality. The terms $s_0 = (k^{\text{S}}_{0,\text{off}}/k^{\text{P}}_{0,\text{off}})$ and $s_1 = (k^{\text{S}}_{1,\text{off}}/k^{\text{P}}_{1,\text{off}})$ parametrize the specificities of the ring for binding/release of substrate and product depending on whether the ring is free in solution (state 0) or on the dumbbell (states 1, 2). If $s_0 \gg 1$ and $s_1 \ll 1$, the most likely sequence when $\Delta\mu > 0$ involves binding of substrate while the ring is off the dumbbell, and then releasing product when the ring is on the dumbbell, thereby trapping the MIM kinetically.

As expected, the ratio is $e^{-\Delta G_{\text{out}}}$ when $\Delta\mu = 0$, but the ratio is also $e^{-\Delta G_{\text{out}}}$ when $s_0 = s_1$. Remarkably, the ratio P_2/P_0 is independent of ΔG and ΔG^*. This point is an important one with regard to designing synthetic autonomous molecular motors: the key is to design allosteric interactions such that part of the driving reaction takes place in one mechanical state and other parts take place in different mechanical states. The interleaving of the chemical and pumping transitions evident in the information ratchet is very much in keeping with the mechanism for ion pumping discussed[82] by Jencks in which the chemical transitions of ATP hydrolysis interleave with the ion binding/release reactions by which an ion is transported across a cell membrane. Jencks mechanism for a molecular pump is in stark contrast to the typical description[83] of molecular motors such as kinesin and myosin in terms of power strokes.

Energy-releasing mechanical transitions, such as $0^* \rightarrow 1^*$ and $1 \rightarrow 2$ in Figure 13, are often termed power-strokes in the biomolecular motor literature.[83] For energy ratchets, the free energies, ΔG and ΔG^*, released in these processes do in fact control the ability of the system to harvest free energy from external fluctuations or from light to maintain a nonequilibrium stationary state. When the energy-supplying process involves the catalysis of an exergonic reaction, however, the constraints of microscopic reversibility reveal that the parameters that characterize the power stroke, namely, ΔG and ΔG^*, are irrelevant for the function of the motor.[84] Put bluntly, a power stroke is not critical to the function of any chemically driven molecular motor even though this paradigm remains the most common one discussed in textbooks. Instead, all chemically driven biomolecular motors function as information ratchets where allosteric interactions provide a mechanism by which the chemical specificities depend on the mechanical state of the motor in such a way that the mechanical or pumping steps are interleaved with the chemical transitions.

CONCLUSIONS AND OUTLOOK

We have designed and tested a wholly synthetic molecular motor that works in a nonreciprocal manner under kinetic control. The optimized design, reached in several highly researched incremental steps, allows the functioning unit to pump repetitively, through redox chemical energy inputs, tetracationic rings from bulk solution to a ring-collecting chain that offers little or no

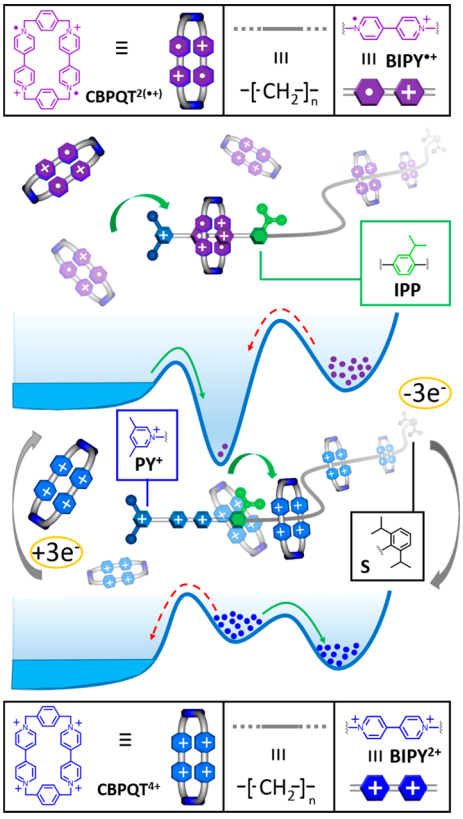

Figure 14. A blueprint for an artificial molecular pump which acts to compartmentalize rings in a high energy state on a polymethylene chain. A graphical representation of a postulated flashing energy ratchet mechanism summarizes how redox chemistry can be employed to prime the pump with rings (top) under reducing conditions and then have it pump the rings (bottom) under oxidative conditions into high energy states. Structural formulas define (top) the $CBPQT^{2(\bullet+)}$ ring and the $BIPY^{\bullet+}$ unit involved in priming the pump and (bottom) the $CBPQT^{4+}$ ring and $BIPY^{2+}$ which give rise to the Coulombic repulsion that pumps the rings onto the polymethylene chain. The structural formulas of the charged (PY^{+}) and neutral (S) stoppers are defined along with that (IPP) of the "steric speed bump" inside blue, black, and green boxes, respectively. Hypothetical distributions of the components of the pump on a simplified potential energy surface diagram are indicated by purple dots in the reduced state and blue in the oxidized state. A solid green arrow indicates a surmountable energy barrier, while the dashed red arrow indicates an insurmountable one.

binding affinity for the rings. The use of chemical reagents is not all that efficient for this energy ratchet system, considering the complexity of the step-wise procedure, not to mention the generation of waste products. The pump would benefit from being operated autonomously using light or an electrochemical input. Given a more efficient mode of operation, we would relish the opportunity of extending (Figure 14) the ring-collecting chain to polymer dimensions so as to be able to trap multiple rings. The prospect of designing a polyrotaxane synthesizer that produces enthalpically and entropically demanding polymers is a seductive one.

A future beckons for the advent of yet more highly sophisticated artificial molecular machines that not only perform work on their surroundings, but also operate dissipatively, far-from-equilibrium in repetitive and progressive ways.[3,85] With the long-term goal of creating a mimetic of Nature's carrier proteins, the next objective will be to anchor artificial molecular pumps at the interface between two surfaces, *e.g.*, in a membrane in order to achieve transmembrane transport, similar to the action of carrier proteins in biological systems. We appreciate, however, that the unidirectional transport of rings along a dumbbell in a membrane is likely to involve much larger energies of activation than the transport of ions and molecules through a channel-like supramolecular superstructure. It is for this reason that we have settled, for the immediate future, on attaching long chains to the opposite end from the pump portion of the motor molecule, leading to a restrained environment that is isolated from bulk solution. Presently, we are engaged in making these high-energy entropically demanding polyrotaxanes[86,87] as surrogates of cellular compartmentalization.

In relation to advancing the science of artificial molecular motors, the next important step will be the development of our synthetic ability to control specificities using allosteric interactions.[49,88] A beginning to this endeavor has been provided by Flood[89,90] in his design of a bilabile switch where the pathway going between switch states depends on the external conditions. Recently, Leigh[91,92] has discussed mechanisms for turning catalytic functions off or on by moving a ring from one recognition site to another. What is necessary for an autonomously driven molecular motor is similar but distinct: the essential idea would be to switch the rates of binding/release of substrate and product between fast binding/release of substrate and slow binding/release of product at one recognition site to fast binding/release of product and slow binding/release of substrate at another recognition site.

The importance of allosteric feedback highlights the role of information in controlling, and even driving, mechanical processes at the molecular scale. One of the surprising conclusions arising from a consideration of the constraints imposed by microscopic reversibility is the irrelevance of the so-called "power-stroke" for determining the directionality and thermodynamics of operation of chemically driven molecular machines. Instead, we see that the next important synthetic goal in the design of molecular motors that imitate biological motors and pumps will be to incorporate allosteric interactions into the wholly synthetic motors in order to drive switching of bilabile specificities so that the rates of binding/release of the fuel and product molecules depend on the position or mechanical state of the machine.

While the ultimate goal is the creation of wholly synthetic molecular machines as complex and versatile as those that have arisen from millions of years of evolution in biological systems, the journey toward this

goal doubtlessly will result in the creation of remarkable tools for harnessing the potential of molecule-by-molecule assembly, as well as leading to an ever-increasing understanding of how biological molecular machines carry out their functions.

Conflict of Interest: The authors declare no competing financial interest.

Acknowledgment. The research described in this review was supported by a grant (CHE-1308107) from the National Science Foundation. P.R.M. thanks the U.S.–U.K. Fulbright Commission for an All-Disciplines Scholar Award.

REFERENCES AND NOTES

1. Lehn, J.-M. Perspectives in Chemistry - Steps Towards Complex Matter. *Angew. Chem., Int. Ed.* **2013**, *52*, 2836–2850.
2. Kinbara, K.; Aida, T. Toward Intelligent Molecular Machines: Directed Motions of Biological and Artificial Molecules and Assemblies. *Chem. Rev.* **2005**, *105*, 1377–1400.
3. Astumian, R. D. Microscopic Reversibility as the Organizing Principle of Molecular Machines. *Nat. Nanotechnol.* **2012**, *7*, 684–688.
4. Astumian, R. D. Thermodynamics and Kinetics of a Brownian Motor. *Science* **1997**, *276*, 917–922.
5. Vinothkumar, K. R.; Henderson, R. Structures of Membrane Proteins. *Q. Rev. Biophys.* **2010**, *43*, 65–158.
6. Kay, E. R.; Leigh, D. A.; Zerbetto, F. Synthetic Molecular Motors and Mechanical Machines. *Angew. Chem., Int. Ed.* **2007**, *46*, 72–191.
7. von Delius, M.; Geertsema, E. M.; Leigh, D. A. A Synthetic Small Molecule That Can Walk Down a Track. *Nat. Chem.* **2010**, *2*, 96–101.
8. Lewandowski, B.; De Bo, G.; Ward, J. W.; Papmeyer, M.; Kuschel, S.; Aldegunde, M. J.; Gramlich, P. M. E.; Heckmann, D.; Goldup, S. M.; D'Souza, D. M.; Fernandes, A. E.; Leigh, D. A. Sequence-Specific Peptide Synthesis by an Artificial Small-Molecule Machine. *Science* **2013**, *339*, 189–193.
9. Vogelsberg, C. S.; Garcia-Garibay, M. A. Crystalline Molecular Machines: Function, Phase Order, Dimensionality, and Composition. *Chem. Soc. Rev.* **2012**, *41*, 1892–1910.
10. Michl, J.; Sykes, E. C. H. Molecular Rotors and Motors: Recent Advances and Future Challenges. *ACS Nano* **2009**, *3*, 1042–1048.
11. Gu, H. Z.; Chao, J.; Xiao, S. J.; Seeman, N. C. A Proximity-Based Programmable DNA Nanoscale Assembly Line. *Nature* **2010**, *465*, 202–206.
12. He, Y.; Liu, D. R. Autonomous Multistep Organic Synthesis in a Single Isothermal Solution Mediated by a DNA Walker. *Nat. Nanotechnol.* **2010**, *5*, 778–782.
13. Pavlick, R. A.; Sengupta, S.; McFadden, T.; Zhang, H.; Sen, A. A Polymerization-Powered Motor. *Angew. Chem., Int. Ed.* **2011**, *50*, 9374–9377.
14. Tierney, H. L.; Murphy, C. J.; Jewell, A. D.; Baber, A. E.; Iski, E. V.; Khodaverdian, H. Y.; McGuire, A. F.; Klebanov, N.; Sykes, E. C. H. Experimental Demonstration of a Single-Molecule Electric Motor. *Nat. Nanotechnol.* **2011**, *6*, 625–629.
15. Coskun, A.; Banaszak, M.; Astumian, R. D.; Stoddart, J. F.; Grzybowski, B. A. Great Expectations: Can Artificial Molecular Machines Deliver on Their Promise?. *Chem. Soc. Rev.* **2012**, *41*, 19–30.
16. Ragazzon, G.; Baroncini, M.; Silvi, S.; Venturi, M.; Credi, A. Light-Powered Autonomous and Directional Molecular Motion of a Dissipative Self-Assembling System. *Nat. Nanotechnol.* **2015**, *10*, 70–75.
17. Feringa, B. L. The Art of Building Small: From Molecular Switches to Molecular Motors. *J. Org. Chem.* **2007**, *72*, 6635–6652.
18. Greb, L.; Lehn, J.-M. Light-Driven Molecular Motors: Imines as Four-Step or Two-Step Unidirectional Rotors. *J. Am. Chem. Soc.* **2014**, *136*, 13114–13117.
19. Bruns, C. J.; Stoddart, J. F. Rotaxane-Based Molecular Muscles. *Acc. Chem. Res.* **2014**, *47*, 2186–2199.
20. Eelkema, R.; Pollard, M. M.; Vicario, J.; Katsonis, N.; Ramon, B. S.; Bastiaansen, C. W. M.; Broer, D. J.; Feringa, B. L. Nanomotor Rotates Microscale Objects. *Nature* **2006**, *440*, 163–163.
21. Li, Q.; Fuks, G.; Moulin, E.; Maaloum, M.; Rawiso, M.; Kulic, I.; Foy, J. T.; Giuseppone, N. Macroscopic Contraction of a Gel Induced by the Integrated Motion of Light-Driven Molecular Motors. *Nat. Nanotechnol.* **2015**, *10*, 161–165.
22. Browne, W. R.; Feringa, B. L. Making Molecular Machines Work. *Nat. Nanotechnol.* **2006**, *1*, 25–35.
23. Berná, J.; Leigh, D. A.; Lubomska, M.; Mendoza, S. M.; Pérez, E. M.; Rudolf, P.; Teobaldi, G.; Zerbetto, F. Macroscopic Transport by Synthetic Molecular Machines. *Nat. Mater.* **2005**, *4*, 704–710.
24. Lussis, P.; Svaldo-Lanero, T.; Bertocco, A.; Fustin, C. A.; Leigh, D. A.; Duwez, A. S. A Single Synthetic Small Molecule That Generates Force against a Load. *Nat. Nanotechnol.* **2011**, *6*, 553–557.
25. Kudernac, T.; Ruangsupapichat, N.; Parschau, M.; Macia, B.; Katsonis, N.; Harutyunyan, S. R.; Ernst, K. H.; Feringa, B. L. Electrically Driven Directional Motion of a Four-Wheeled Molecule on a Metal Surface. *Nature* **2011**, *479*, 208–211.
26. van Dongen, S. F. M.; Cantekin, S.; Elemans, J. A. A. W.; Rowan, A. E.; Nolte, R. J. M. Functional Interlocked Systems. *Chem. Soc. Rev.* **2014**, *43*, 99–122.
27. van Dongen, S. F. M.; Elemans, J. A. A. W.; Rowan, A. E.; Nolte, R. J. M. Processive Catalysis. *Angew. Chem., Int. Ed.* **2014**, *53*, 11420–11428.
28. Bissell, R. A.; Córdova, E.; Kaifer, A. E.; Stoddart, J. F. A Chemically and Electrochemically Switchable Molecular Shuttle. *Nature* **1994**, *369*, 133–137.
29. Stoddart, J. F. The Chemistry of the Mechanical Bond. *Chem. Soc. Rev.* **2009**, *38*, 1802–1820.
30. Asakawa, M.; Ashton, P. R.; Balzani, V.; Credi, A.; Hamers, C.; Mattersteig, G.; Montalti, M.; Shipway, A. N.; Spencer, N.; Stoddart, J. F.; Tolley, M. S.; Venturi, M.; White, A. J. P.; Williams, D. J. A Chemically and Electrochemically Switchable [2]Catenane Incorporating a Tetrathiafulvalene Unit. *Angew. Chem., Int. Ed.* **1998**, *37*, 333–337.
31. Collier, C. P.; Mattersteig, G.; Wong, E. W.; Luo, Y.; Beverly, K.; Sampaio, J.; Raymo, F. M.; Stoddart, J. F.; Heath, J. R. A [2]Catenane-Based Solid State Electronically Reconfigurable Switch. *Science* **2000**, *289*, 1172–1175.
32. Liu, Y.; Flood, A. H.; Bonvallett, P. A.; Vignon, S. A.; Northrop, B. H.; Tseng, H. R.; Jeppesen, J. O.; Huang, T. J.; Brough, B.; Baller, M.; Magonov, S.; Solares, S. D.; Goddard, W. A.; Ho, C. M.; Stoddart, J. F. Linear Artificial Molecular Muscles. *J. Am. Chem. Soc.* **2005**, *127*, 9745–9759.
33. Anelli, P.-L.; Spencer, N.; Stoddart, J. F. A Molecular Shuttle. *J. Am. Chem. Soc.* **1991**, *113*, 5131–5133.
34. Fahrenbach, A. C.; Barnes, J. C.; Li, H.; Benítez, D.; Basuray, A. N.; Fang, L.; Sue, C. H.; Barin, G.; Dey, S. K.; Goddard, W. A.; Stoddart, J. F. Measurement of the Ground-State Distributions in Bistable Mechanically Interlocked Molecules Using Slow Scan Rate Cyclic Voltammetry. *Proc. Natl. Acad. Sci. U. S. A.* **2011**, *108*, 20416–20421.
35. Fahrenbach, A. C.; Bruns, C. J.; Li, H.; Trabolsi, A.; Coskun, A.; Stoddart, J. F. Ground-State Kinetics of Bistable Redox-Active Donor-Acceptor Mechanically Interlocked Molecules. *Acc. Chem. Res.* **2014**, *47*, 482–493.
36. Coskun, A.; Spruell, J. M.; Barin, G.; Dichtel, W. R.; Flood, A. H.; Botros, Y. Y.; Stoddart, J. F. High Hopes: Can Molecular Electronics Realise Its Potential? *Chem. Soc. Rev.* **2012**, *41*, 4827–4859.
37. Li, Z. X.; Barnes, J. C.; Bosoy, A.; Stoddart, J. F.; Zink, J. I. Mesoporous Silica Nanoparticles in Biomedical Applications. *Chem. Soc. Rev.* **2012**, *41*, 2590–2605.
38. Ceroni, P.; Credi, A.; Venturi, M. Light to Investigate (Read) and Operate (Write) Molecular Devices and Machines. *Chem. Soc. Rev.* **2014**, *43*, 4068–4083.
39. Caballero, A.; Zapata, F.; Beer, P. D. Interlocked Host Molecules for Anion Recognition and Sensing. *Coord. Chem. Rev.* **2013**, *257*, 2434–2455.

40. Green, J. E.; Choi, J. W.; Boukai, A.; Bunimovich, Y.; Johnston-Halperin, E.; Delonno, E.; Luo, Y.; Sheriff, B. A.; Xu, K.; Shin, Y. S.; Tseng, H. R.; Stoddart, J. F.; Heath, J. R. A 160-Kilobit Molecular Electronic Memory Patterned at 10^{11} Bits Per Square Centimetre. *Nature* **2007**, *445*, 414–417.
41. Bakalis, E.; Zerbetto, F. Are Two-Station Biased Random Walkers Always Potential Molecular Motors? *ChemPhysChem* **2015**, *16*, 104–107.
42. Badjić, J. D.; Balzani, V.; Credi, A.; Silvi, S.; Stoddart, J. F. A Molecular Elevator. *Science* **2004**, *303*, 1845–1849.
43. McGonigal, P. R.; Li, H.; Cheng, C.; Schneebeli, S. T.; Frasconi, M.; Witus, L. S.; Stoddart, J. F. Controlling Association Kinetics in the Formation of Donor−Acceptor Pseudorotaxanes. *Tetrahedron Lett.* **2015**, *56*, 3591–3594.
44. Trabolsi, A.; Khashab, N.; Fahrenbach, A. C.; Friedman, D. C.; Colvin, M. T.; Coti, K. K.; Benítez, D.; Tkatchouk, E.; Olsen, J. C.; Belowich, M. E.; Carmielli, R.; Khatib, H. A.; Goddard, W. A.; Wasielewski, M. R.; Stoddart, J. F. Radically Enhanced Molecular Recognition. *Nat. Chem.* **2010**, *2*, 42–49.
45. Fahrenbach, A. C.; Barnes, J. C.; Lanfranchi, D. A.; Li, H.; Coskun, A.; Gassensmith, J. J.; Liu, Z. C.; Benítez, D.; Trabolsi, A.; Goddard, W. A.; Elhabiri, M.; Stoddart, J. F. Solution-Phase Mechanistic Study and Solid-State Structure of a Tris(Bipyridinium Radical Cation) Inclusion Complex. *J. Am. Chem. Soc.* **2012**, *134*, 3061–3072.
46. Chatterjee, M. N.; Kay, E. R.; Leigh, D. A. Beyond Switches: Ratcheting a Particle Energetically Uphill with a Compartmentalized Molecular Machine. *J. Am. Chem. Soc.* **2006**, *128*, 4058–4073.
47. Serreli, V.; Lee, C. F.; Kay, E. R.; Leigh, D. A. A Molecular Information Ratchet. *Nature* **2007**, *445*, 523–527.
48. Barrell, M. J.; Campaña, A. G.; von Delius, M.; Geertsema, E. M.; Leigh, D. A. Light-Driven Transport of a Molecular Walker in Either Direction Along a Molecular Track. *Angew. Chem., Int. Ed.* **2011**, *50*, 285–290.
49. Carlone, A.; Goldup, S. M.; Lebrasseur, N.; Leigh, D. A.; Wilson, A. A Three-Compartment Chemically-Driven Molecular Information Ratchet. *J. Am. Chem. Soc.* **2012**, *134*, 8321–8323.
50. Baroncini, M.; Silvi, S.; Venturi, M.; Credi, A. Photoactivated Directionally Controlled Transit of a Non-Symmetric Molecular Axle through a Macrocycle. *Angew. Chem., Int. Ed.* **2012**, *51*, 4223–4226.
51. Arduini, A.; Bussolati, R.; Credi, A.; Secchi, A.; Silvi, S.; Semeraro, M.; Venturi, M. Toward Directionally Controlled Molecular Motions and Kinetic Intra- and Intermolecular Self-Sorting: Threading Processes of Nonsymmetric Wheel and Axle Components. *J. Am. Chem. Soc.* **2013**, *135*, 9924–9930.
52. Coskun, A.; Friedman, D. C.; Li, H.; Patel, K.; Khatib, H. A.; Stoddart, J. F. A Light-Gated Stop-Go Molecular Shuttle. *J. Am. Chem. Soc.* **2009**, *131*, 2493–2495.
53. Avellini, T.; Li, H.; Coskun, A.; Barin, G.; Trabolsi, A.; Basuray, A. N.; Dey, S. K.; Credi, A.; Silvi, S.; Stoddart, J. F.; Venturi, M. Photoinduced Memory Effect in a Redox Controllable Bistable Mechanical Molecular Switch. *Angew. Chem., Int. Ed.* **2012**, *51*, 1611–1615.
54. Hmadeh, M.; Fahrenbach, A. C.; Basu, S.; Trabolsi, A.; Benítez, D.; Li, H.; Albrecht-Gary, A. M.; Elhabiri, M.; Stoddart, J. F. Electrostatic Barriers in Rotaxanes and Pseudorotaxanes. *Chem. - Eur. J.* **2011**, *17*, 6076–6087.
55. Li, H.; Cheng, C. Y.; McGonigal, P. R.; Fahrenbach, A. C.; Frasconi, M.; Liu, W. G.; Zhu, Z. X.; Zhao, Y. L.; Ke, C. F.; Lei, J. Y.; Young, R. M.; Dyar, S. M.; Co, D. T.; Yang, Y. W.; Botros, Y. Y.; Goddard, W. A.; Wasielewski, M. R.; Astumian, R. D.; Stoddart, J. F. Relative Unidirectional Translation in an Artificial Molecular Assembly Fueled by Light. *J. Am. Chem. Soc.* **2013**, *135*, 18609–18620.
56. Kundu, P. K.; Klajn, R. Watching Single Molecules Move in Response to Light. *ACS Nano* **2014**, *8*, 11913–11916.
57. Balzani, V.; Clemente-Leon, M.; Credi, A.; Ferrer, B.; Venturi, M.; Flood, A. H.; Stoddart, J. F. Autonomous Artificial Nanomotor Powered by Sunlight. *Proc. Natl. Acad. Sci. U. S. A.* **2006**, *103*, 1178–1183.
58. Li, H.; Zhu, Z. X.; Fahrenbach, A. C.; Savoie, B. M.; Ke, C. F.; Barnes, J. C.; Lei, J. Y.; Zhao, Y. L.; Lilley, L. M.; Marks, T. J.; Ratner, M. A.; Stoddart, J. F. Mechanical Bond-Induced Radical Stabilization. *J. Am. Chem. Soc.* **2013**, *135*, 456–467.
59. Kosower, E. M.; Cotter, J. L. Stable Free Radicals 0.2. Reduction of 1-Methyl-4-Cyanopyridinium Ion to Methylviologen Cation Radical. *J. Am. Chem. Soc.* **1964**, *86*, 5524–5527.
60. Hünig, S. Stable Radical Ions. *Pure Appl. Chem.* **1967**, *15*, 109–122.
61. Cheng, C. Y.; McGonigal, P. R.; Liu, W. G.; Li, H.; Vermeulen, N. A.; Ke, C. F.; Frasconi, M.; Stern, C. L.; Goddard, W. A.; Stoddart, J. F. Energetically Demanding Transport in a Supramolecular Assembly. *J. Am. Chem. Soc.* **2014**, *136*, 14702–14705.
62. Makita, Y.; Kihara, N.; Takata, T. Quantitative Active Transport in [2]Rotaxane Using a One-Shot Acylation Reaction toward the Linear Molecular Motor. *J. Org. Chem.* **2008**, *73*, 9245–9250.
63. Nishiyama, J.; Makita, Y.; Kihara, N. The Cyclopentyl Group, as a Small but Bulky Terminal Group, Allows Rapid and Efficient Active Transport. *Org. Lett.* **2015**, *17*, 138–141.
64. Ashton, P. R.; Baxter, I.; Fyfe, M. C. T.; Raymo, F. M.; Spencer, N.; Stoddart, J. F.; White, A. J. P.; Williams, D. J. Rotaxane or Pseudorotaxane? That Is the Question! *J. Am. Chem. Soc.* **1998**, *120*, 2297–2307.
65. Conyard, J.; Cnossen, A.; Browne, W. R.; Feringa, B. L.; Meech, S. R. Chemically Optimizing Operational Efficiency of Molecular Rotary Motors. *J. Am. Chem. Soc.* **2014**, *136*, 9692–9700.
66. Cheng, C.; McGonigal, P. R.; Schneebeli, S. T.; Li, H.; Vermeulen, N. A.; Ke, C.; Stoddart, J. F. An Artificial Molecular Pump. *Nat. Nanotechnol.* **2015**, *10*, 547–553.
67. Sevick, E. M.; Williams, D. R. M. Piston-Rotaxanes as Molecular Shock Absorbers. *Langmuir* **2010**, *26*, 5864–5868.
68. Sevick, E. M.; Williams, D. R. M. A Piston-Rotaxane with Two Potential Stripes: Force Transitions and Yield Stresses. *Molecules* **2013**, *18*, 13398–13409.
69. Goldup, S. Artificial Molecular Machines: Two Steps Uphill. *Nat. Nanotechnol.* **2015**, *10*, 488–489.
70. Steinberg-Yfrach, G.; Liddell, P. A.; Hung, S. C.; Moore, A. L.; Gust, D.; Moore, T. A. Conversion of Light Energy to Proton Potential in Liposomes by Artificial Photosynthetic Reaction Centres. *Nature* **1997**, *385*, 239–241.
71. Bennett, I. M.; Farfano, H. M. V.; Bogani, F.; Primak, A.; Liddell, P. A.; Otero, L.; Sereno, L.; Silber, J. J.; Moore, A. L.; Moore, T. A.; Gust, D. Active Transport of Ca^{2+} by an Artificial Photosynthetic Membrane. *Nature* **2002**, *420*, 398–401.
72. Bhosale, S.; Sisson, A. L.; Talukdar, P.; Furstenberg, A.; Banerji, N.; Vauthey, E.; Bollot, G.; Mareda, J.; Roger, C.; Wurthner, F.; Sakai, N.; Matile, S. Photoproduction of Proton Gradients with Pi-Stacked Fluorophore Scaffolds in Lipid Bilayers. *Science* **2006**, *313*, 84–86.
73. Xie, X. J.; Crespo, G. A.; Mistlberger, G.; Bakker, E. Photocurrent Generation Based on a Light-Driven Proton Pump in an Artificial Liquid Membrane. *Nat. Chem.* **2014**, *6*, 202–207.
74. Hirokawa, N.; Noda, Y.; Tanaka, Y.; Niwa, S. Kinesin Superfamily Motor Proteins and Intracellular Transport. *Nat. Rev. Mol. Cell Biol.* **2009**, *10*, 682–696.
75. Adelstein, R. S.; Eisenberg, E. Regulation and Kinetics of the Actin-Myosin-ATP Interaction. *Annu. Rev. Biochem.* **1980**, *49*, 921–956.
76. Boyer, P. D. The ATP Synthase — A Splendid Molecular Machine. *Annu. Rev. Biochem.* **1997**, *66*, 717–749.
77. Wadhams, G. H.; Armitage, J. P. Making Sense of It All: Bacterial Chemotaxis. *Nat. Rev. Mol. Cell Biol.* **2004**, *5*, 1024–1037.
78. Astumian, R. D. Huxley's Model for Muscle Contraction Revisited: the Importance of Microscopic Reversibility. *Top. Curr. Chem.* **2015**, 10.1007/128_2015_644.
79. Astumian, R. D.; Derényi, I. Fluctuation Driven Transport and Models of Molecular Motors and Pumps. *Eur. Biophys. J.* **1998**, *27*, 474–489.
80. Astumian, R. D.; Chock, P. B.; Tsong, T. Y.; Chen, Y. D.; Westerhoff, H. V. Can Free Energy Be Transduced From Electric Noise? *Proc. Natl. Acad. Sci. U. S. A.* **1987**, *84*, 434–438.

81. Leigh, D. A.; Wong, J. K. Y.; Dehez, F.; Zerbetto, F. Unidirectional Rotation in a Mechanically Interlocked Molecular Rotor. *Nature* **2003**, *424*, 174–179.
82. Jencks, W. P.; Yang, T.; Peisach, D.; Myung, J. Calcium ATPase of Sarcoplasmic Reticulum has Four Binding Sites for Calcium. *Biochemistry* **1993**, *32*, 7030–7034.
83. Vale, R. D.; Milligan, R. A. The Way Things Move: Looking under the Hood of Molecular Motor Proteins. *Science* **2000**, *288*, 88–95.
84. Astumian, R. D. Irrelevance of the Power Stroke for the Directionality, Stopping Force, and Optimal Efficiency of Chemically Driven Molecular Machines. *Biophys. J.* **2015**, *108*, 291–303.
85. Abendroth, J. M.; Bushuyev, O. S.; Weiss, P. S.; Barrett, C. J. Controlling Motion at the Nanoscale: Rise of the Molecular Machines. *ACS Nano* **2015**, 10.1021/acsnano.5b03367.
86. Bin Imran, A.; Esaki, K.; Gotoh, H.; Seki, T.; Ito, K.; Sakai, Y.; Takeoka, Y. Extremely Stretchable Thermosensitive Hydrogels by Introducing Slide-Ring Polyrotaxane Cross-Linkers and Ionic Groups into the Polymer Network. *Nat. Commun.* **2014**, *5*, 5124.
87. Noda, Y.; Hayashi, Y.; Ito, K. From Topological Gels to Slide-Ring Materials. *J. Appl. Polym. Sci.* **2014**, *131*, 40509.
88. Alvarez-Pérez, M.; Goldup, S. M.; Leigh, D. A.; Slawin, A. M. Z. A Chemically-Driven Infromation Ratchet. *J. Am. Chem. Soc.* **2008**, *130*, 1836–1838.
89. Share, A. I.; Parimal, K.; Flood, A. H. Bilability Is Defined When One Electron Is Used to Switch Between Concerted and Stepwise Pathways in Cu(I)-Based Bistable [2/3]Pseudorotaxanes. *J. Am. Chem. Soc.* **2010**, *132*, 1665–1675.
90. Qiao, B.; Sengupta, A.; Liu, Y.; McDonald, K. P.; Pink, M.; Anderson, J. R.; Raghavachari, K.; Flood, A. H. Electrostatic and Allosteric Cooperativity in Ion-Pair Binding: A Quantitative and Coupled Experiment−Theory Study with Aryl−Triazole−Ether Macrocycles. *J. Am. Chem. Soc.* **2015**, 10.1021/jacs.5b05839.
91. Beswick, J.; Blanco, V.; De Bo, G.; Leigh, D. A.; Lewandowska, U.; Lewandowski, B.; Mishiro, K. Selecting Reactions and Reactants Using a Switchable Rotaxane Organocatalyst with Two Different Active Sites. *Chem. Sci.* **2015**, *6*, 140–143.
92. Blanco, V.; Leigh, D. A.; Marcos, V. Artificial Switchable Catalysts. *Chem. Soc. Rev.* **2015**, *44*, 5341–5370.